Article

Neuron

Tentonin 3/TMEM150c Confers Distinct Mechanosensitive Currents in Dorsal-Root Ganglion Neurons with Proprioceptive Function

Highlights

- Tentonin 3 (TTN3) is activated by mechanical stimuli with slow inactivation kinetics
- Ablation of TTN3 reduces slow-adapting mechanosensitive currents in DRG neurons
- TTN3 currents are blocked by well-known blockers of mechanosensitive channels
- TTN3 is localized in muscle spindles and contributes to proprioception

Authors

Gyu-Sang Hong, Byeongjun Lee, Jungwon Wee, ..., Gyu Hyun Kim, In-Beom Kim, Uhtaek Oh

Correspondence

utoh@snu.ac.kr

In Brief

Mechanosensation is a fundamental function required for the survival of vertebrates. Mechanosensation is mediated by mechanotransduction channels. Hong et al. found that Tentonin 3 (TMEM150C) is a new class of mechanotransduction channel. Surprisingly, TTN3 is expressed in muscle spindle afferents. Because genetic ablation of TTN3 reduces motor coordination, TTN3 appears to contribute to proprioception. Thus, cloning of TTN3 leads to understanding of various other mechanotransduction mechanisms

Hong et al., 2016, Neuron *91*, 107–118
July 6, 2016
http://dx.doi.org/10.1016/j.neuron.2016.05.029

CellPress

Neuron
Article

Tentonin 3/TMEM150c Confers Distinct Mechanosensitive Currents in Dorsal-Root Ganglion Neurons with Proprioceptive Function

Gyu-Sang Hong,[1,4] Byeongjun Lee,[1,4] Jungwon Wee,[1] Hyeyeon Chun,[2] Hyungsup Kim,[2] Jooyoung Jung,[2] Joo Young Cha,[2] Tae-Ryong Riew,[3] Gyu Hyun Kim,[3] In-Beom Kim,[3] and Uhtaek Oh[1,2,*]
[1]Department of Molecular Medicine and Biopharmaceutical Sciences, Graduate School of Convergence Science and Technology, Seoul National University, Gyunggy 16229, Korea
[2]Sensory Research Center, CRI, College of Pharmacy, Seoul National University, Seoul 08826, Korea
[3]Department of Anatomy, Catholic Neuroscience Institute, College of Medicine, Catholic University, Seoul 06591, Korea
[4]Co-first author
*Correspondence: utoh@snu.ac.kr
http://dx.doi.org/10.1016/j.neuron.2016.05.029

SUMMARY

Touch sensation or proprioception requires the transduction of mechanical stimuli into electrical signals by mechanoreceptors in the periphery. These mechanoreceptors are equipped with various transducer channels. Although Piezo1 and 2 are mechanically activated (MA) channels with rapid inactivation, MA molecules with other inactivation kinetics have not been identified. Here we report that heterologously expressed Tentonin3 (TTN3)/TMEM150C is activated by mechanical stimuli with distinctly slow inactivation kinetics. Genetic ablation of *Ttn3/Tmem150c* markedly reduced slowly adapting neurons in dorsal-root ganglion neurons. The MA TTN3 currents were inhibited by known blockers of mechanosensitive ion channels. Moreover, TTN3 was localized in muscle spindle afferents. *Ttn3*-deficient mice exhibited the loss of coordinated movements and abnormal gait. Thus, TTN3 appears to be a component of a mechanosensitive channel with a slow inactivation rate and contributes to motor coordination. Identification of this gene advances our understanding of the various types of mechanosensations, including proprioception.

INTRODUCTION

Mechanosensation, the sensation of external and internal mechanical stimuli, is essential for the survival of animals. In mammals, it is required for tactile sensation, proprioception, and nociception (Delmas and Coste, 2013). Proprioception is a sense of limb position and movement. Proprioceptive sensory signals are essential for coordinated movements, including locomotion (Akay et al., 2014; de Nooij et al., 2015; Proske and Gandevia, 2012). Proprioception involves sensory inputs from muscles, skin, joints, and tendons. Among these sensory inputs, muscle spindle (MS) afferents play a key role in proprioception (Proske and Gandevia, 2012; Rossi-Durand, 2006). MS is composed of encapsulated intrafusal muscle fibers that are innervated with group Ia and II sensory afferents (Barker, 1974; Proske and Gandevia, 2012; Rossi-Durand, 2006). MS afferents project to the ventral horn of the spinal cord, where they connect monosynaptically to motor neurons or interneurons to transmit signals to brain (Hunt, 1974; Proske and Gandevia, 2012). They are sensitive to passive muscle stretch or during contraction (Banks, 1994; Bewick and Banks, 2015; Hunt, 1974). Thus, the neural responses of MS afferents to muscle stretch are key signals to coordinate body movements (Proske and Gandevia, 2012). Deafferentation or genetic disruption of MS induces neurological deficits such as gait ataxia with loss of central pattern generation of locomotion (Akay et al., 2014; Cheret et al., 2013; de Nooij et al., 2015; Tourtellotte and Milbrandt, 1998). In addition, changes in proprioception, such as fatigue after exhaustive exercise, aging, and Parkinson's disease, often lead to injury due to loss of motor coordination (Proske and Gandevia, 2012).

The molecular identity of mechanotransduction channels has long been sought. Large conductance mechanosensitive channels generate mechanosensitive currents in *Escherichia coli,* functioning as an osmotic valve in the bacteria (Levina et al., 1999; Sukharev et al., 1994). The DEG/epithelium sodium channel (ENaC) and NOMPC families are components of the mechanotransduction channel in the mechanosensory neurons of *Caenorhabditis elegans* and *Drosophila melanogaster* (Huang and Chalfie, 1994; O'Hagan et al., 2005; Walker et al., 2000). However, these channels are not found in mammals (Chalfie, 2009). In addition, mechanical gating of these channels in heterologously expressed cells was not achieved. Piezo1 and 2, which are found in mammals and other species of the animal kingdom, are activated by mechanical force (Coste et al., 2010). Piezo2 is present in Merkel cells and cutaneous nerves in the skin, suggesting a role for tactile sensation. Indeed, genetic disruption of Piezo2 in dorsal-root ganglion (DRG) neurons and Merkel cells markedly reduced rapidly adapting mechanically activated (MA) currents, low-threshold mechanoreceptor responses in the skin, and touch sensation in vivo (Ikeda et al., 2014; Ranade et al., 2014b; Woo et al., 2014). In addition, Piezo1 appears to be essential for the development and maintenance of vascular architecture (Li et al., 2014; Ranade et al., 2014a). Thus,

Piezo channels are involved in tactile sensation and stress-mediated cellular responses. Recently, Piezo2 has been shown to play a key role in proprioception. Woo et al. (2015) found that Piezo2 is present in MSs, and its genetic deletion from muscle afferents leads to marked reduction in stretch-induced nerve activity of MS afferents as well as prominent loss of muscle coordination (Woo et al., 2015).

Sensory neurons in DRGs are known to respond to mechanical stimuli with rapidly, slowly, or intermediately inactivating cationic currents (Drew et al., 2002, 2004; Hao and Delmas, 2010; Hu and Lewin, 2006). MS afferents are slowly adapting (SA) as they continue to respond to sustained muscle stretch (de Nooij et al., 2015; Hunt, 1974; Hunt and Ottoson, 1975). As Piezo2 in DRG neurons confers rapidly adapting (RA) (inactivating) MA currents, kinetically different MA currents neurons are likely to represent mechanotransduction channels in DRG. Therefore, in the present study we aimed to identify genes conferring kinetically different MA currents from Piezo2 in DRG neurons and test for anatomical and physiological roles in MS afferent activity.

RESULTS

Cloning of Tentonin 3

To find MA channels with slow inactivation kinetics, we performed a bioinformatic investigation (Coste et al., 2010; Yang et al., 2008). We first screened DNA chips (Agilent) after hybridization with RNAs isolated from human DRG cells and six human cell lines; HEK293T, Henrietta Lacks (HeLa), retinal pigment epithelium, human keratinocyte, hepatocellular carcinoma, and human cervical carcinoma cells. We expected that SA MA channels would be found mainly in the DRG neurons. Therefore, we searched for genes in the six human cell lines whose hybridization intensities were less than that of DRG cells. In addition, we filtered out genes of known function or genes encoding five or fewer transmembrane domains. We then transfected Cy3-tagged small interfering RNAs (siRNAs) of the selected candidate genes into isolated DRG neurons from adult mice and tested if they showed a reduction in the SA currents in response to mechanical steps. We found that knockdown of one gene, *Tmem150c*, showed a marked reduction in the amplitude of the SA currents as well as in population of SA-type neurons (see below). We renamed this gene "Tentonin 3" (TTN3) from the Greek "tentono" (τεντωνω), meaning "to stretch."

Activation by Mechanical Stimulation

TTN3 is a relatively small protein with 249 amino acids, predicted to have six transmembrane domains (Figure 1A). A search for orthologs in the animal kingdom revealed that only vertebrates (phylum Chordata) have this gene family. The *Ttn* genes were not found in the lower phyla of the animal kingdom or in plants (Figure 1B). TTN3 appeared to be less related to the other two paralogs, sharing 26.5% and 28.1% sequence identity with TTN1 and TTN2, respectively. In contrast, mouse TTN3 had 96% and 99% amino acid sequence similarity with its human and rat orthologs, respectively.

The majority of TTN3 was observed to be targeted to the plasma membrane when overexpressed heterologously in HEK293T cells (Figure S1). To test its mechanosensitivity, whole-cell currents were recorded from various cell lines transfected with pIRES2-AcGFP1-TTN3. The plasma membrane surface of TTN3-expressing cells was distended with a piezoelectrically driven glass probe. When mechanical steps were applied to the cell, robust currents were activated in HEK293T cells (Figures 1C and 1E; Movie S1). After the rapid activation, these currents showed rapid inactivation, followed by slowly inactivating MA currents, which persisted as long as the mechanical stimuli were sustained. When the mechanical steps were withdrawn, the currents were deactivated, with residual currents persisting for more than several seconds (Figure 1C). The mean current was 975.7 ± 113.8 pA in *Ttn3*-transfected HEK293T cells (Figure 1E). The mechanical steps evoked MA currents greater than 200 pA in 34 of 66 *Ttn*3-transfected HEK293T cells (52%). Only 7 of 45 (16%) *Gfp*-transfected control cells responded to the mechanical steps with small current amplitudes (82.7 ± 12.6 pA, n = 7) and fast inactivation kinetics, consistent with previous research (Coste et al., 2010).

Two homologs, TTN1 (TMEM150A) and TTN2 (TMEM150B), also showed MA currents when expressed in HEK293T cells, but to a much smaller magnitude (Figure 1E). The inactivation time constant (τ_i) was 286.1 ± 41.1 ms (n = 7). The steady-state currents at 600 ms mechanical stimulus were about 52.5% of the peak currents in TTN3/HEK293T cells. Because of the slow inactivation time constants (>30 ms), these TTN3-dependent MA currents were classified as the SA mechanotransduction group observed in DRG neurons (Hao and Delmas, 2010).

F11 is a cell line hybridizing between a mouse neuroblastoma, N18TG-2, and rat DRG neurons (Ghil et al., 2000). F11 cells have a round and large cell soma, like DRG neurons, so that it is easy to apply mechanical step stimuli. Mechanical activation on F11 cells transfected with *Ttn3* also induced MA currents (1,958 ± 194 pA, n = 33) with slow inactivation kinetics (Figures 1D and 1E). Mechanical activation on control F11 cells induced small MA currents (187.9 ± 22.2 pA, n = 19). The mechanical steps evoked MA currents (>200 pA) in 33 of 41 (80%) *Ttn*3-transfected F11 cells. When mechanical steps with variable distances were applied to the surface of the *Ttn*3-transfected F11 cells, graded MA currents were observed (Figures 1D and 1F). The half-maximal distance for activating TTN3 was 4.8 ± 0.2 μm (n = 6), which was similar to that for human Piezo1 (4.7 ± 0.3 μm, n = 6) expressed in F11 cells (Figure 1F). However, the threshold distance (3.2 ± 0.1 μm, n = 6) for activating TTN3 was significantly larger than that for Piezo1 (2.3 ± 0.2 μm, n = 6, $p < 0.01$, Student's t test).

The mechanical steps also induced large MA currents with slow inactivation kinetics in HeLa cells transfected with *Ttn3* (Figure S2). Taken together, TTN3 is activated by mechanical steps when expressed heterologously in various cell types.

TTN3 Is Required for SA MA Currents in DRG Neurons

Mechanical activation of dissociated DRG neurons induced three distinct types of MA currents, RA, intermediately adapting (IA), and SA, with $\tau_i < 10$ ms, $10 < \tau_i < 30$ ms, and $\tau_i > 30$ ms, respectively (Coste et al., 2010; Drew et al., 2004; Hao and Delmas, 2010; Hu and Lewin, 2006) (Figures 2B and 2C). The proportions of RA-, IA-, and SA-type control (transfected with

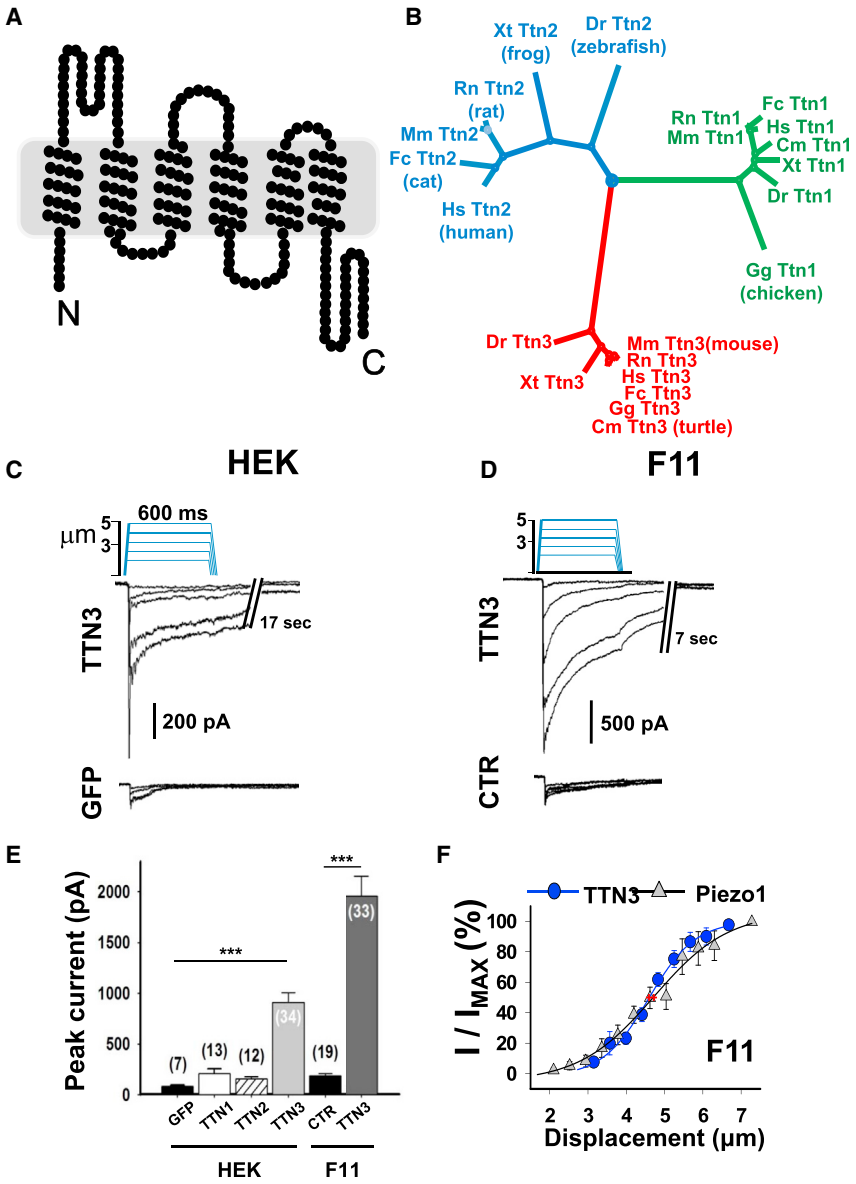

Figure 1. TTN3 Induces MA Currents with Slow Inactivation Kinetics

(A) A putative topology of TTN3 predicted by the TMHMM program. Each dot represents an amino acid in mouse TTN3.

(B) A phylogenetic tree of the *Ttn* gene family among different species in vertebrates (phylum Chordata). The sequence alignment and dendrogram were drawn using the CLUSTALW program. Cm, *Chelonia mydas*; Dr, *Danio rerio*; Fc, *Felis catus*; Gg, *Gallus gallus*; Hs, *Homo sapiens*; Mm, *Mus musculus*; Rn, *Rattus norvegicus*; Xt, *Xenopus tropicalis*.

(C) Representative traces of the currents activated by the mechanical steps in *Ttn3*- and *Gfp*-transfected HEK293T cells. After forming a whole cell, mechanical steps of 600 ms duration were applied to the surface. E_{hold} = −60 mV.

(D) Representative traces of MA currents in *Ttn3*- and cy3-tagged scrambled siRNA (CTR) transfected F11 cells.

(E) Average peak amplitudes of MA currents activated by a 5.0 μm mechanical step in *Ttn1*-, *Ttn2*-, *Ttn3*-, and *Gfp*-transfected HEK293T or scrambled siRNA (CTR) and *Ttn3*-transfected F11 cells. Bars represent SEM. The numbers in parentheses represent the number of cells tested. ***p < 0.001, one-way ANOVA, Tukey's post hoc test.

(F) Displacement-response relationships of TTN3 (circles) and hPiezo1 (triangles) in F11 cells. MA currents (I) were normalized by maximal peak currents (I_{MAX}) activated by displacement of the mechanical stimulation. The mechanical steps were applied for 600 ms. Displacement represents the distance of the mechanical step from the surface of the cell. Normalized currents were fitted to a Boltzmann equation given by I/I_{MAX} (%) = $\{1 + \exp[-(D - D_{1/2})/k]\}^{-1}$, where D is the indentation distance, $D_{1/2}$ is the half-maximal displacement, and k is the response sensitivity to the indentation. Red dots represent the means of $D_{1/2}$ values.

scrambled siRNA) DRG neurons (236 cells) were 41%, 25%, and 22%, respectively. In contrast, when Cy3-tagged *Ttn3* siRNA was transfected to DRG neurons, the proportion of cells with SA MA currents was reduced to 10% (Figure 2C). In order to see a clear phenotype, *Ttn3* knockout (KO) mice were generated (Figure 2A). The proportion of SA-type neurons was dramatically reduced to 4% in *Ttn3* KO DRG neurons (Figures 2B and 2C). Notably, we could not observe SA currents that had inactivation time constants (τ_i) longer than 80 ms in *Ttn3* KO DRG neurons (Figures 2B and 2D). Thus, these results indicate that TTN3 is essential for SA currents in DRG neurons.

Biophysical Property

The steady-state currents of TTN3 induced by mechanical steps of different durations persisted as long as the mechanical stimuli were maintained, up to 1,000 ms (Figure 3A). To test the slow-inactivating kinetics further, a two-step mechanical stimulus protocol was used, consisting of 100 ms conditioning steps with indentations of 2.9–4.6 μm with 0.42 μm increments, followed by a 4.6 μm test step (Figure 3B). Even though the magnitudes of conditioning steps varied, the peak or steady-state MA currents at the test steps did not change (Figures 3B–3D). Thus, a large portion of the MA current still persisted at the test step. These results indicate that some TTN3 are still active even after prolonged mechanical stimuli, which is a property of SA currents found in DRG neurons (Hao and Delmas, 2010).

The current-voltage relationship of the steady-state current was obtained to measure the reversal potential (Figure 3E). The TTN3 MA current was cationic with a reversal potential of 6.7 ± 0.7 mV (n = 9) in 150 mM CsCl and 150 mM NaCl for pipette and bath solutions, respectively. Judging by the reversal

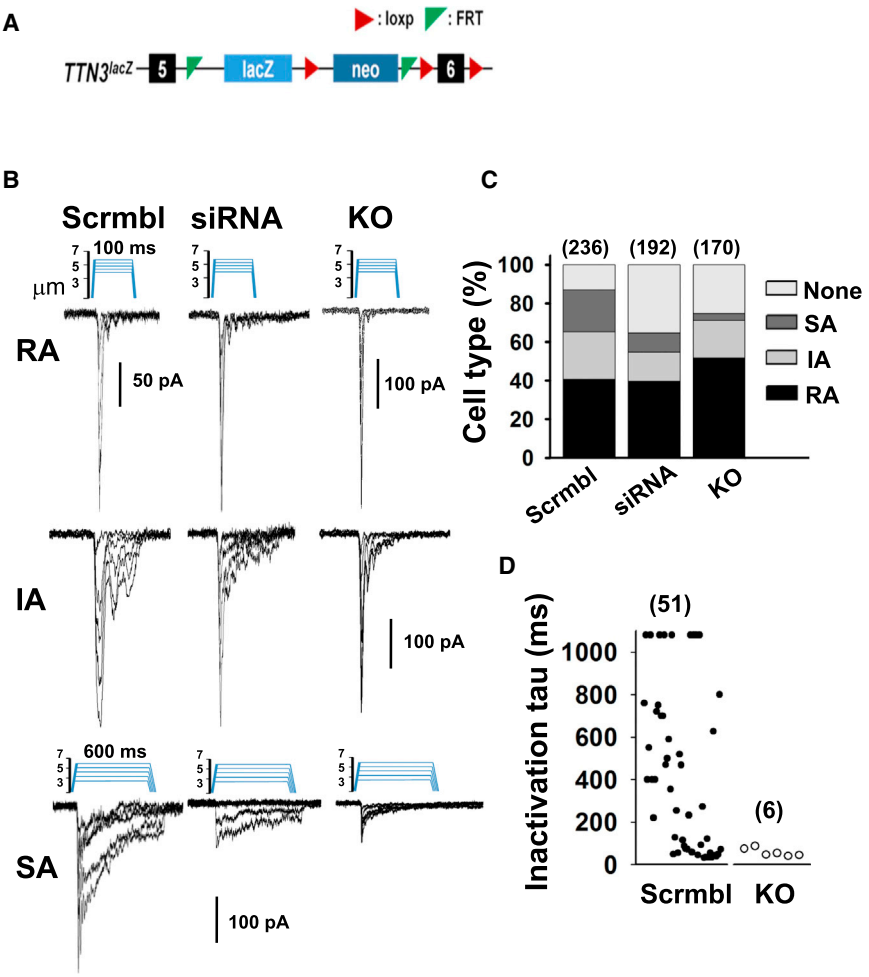

Figure 2. Genetic Ablation of *Ttn3* Reduces the Number of Cells with SA MA Currents in DRG Neurons

(A) Vector construct for gene targeting. Exon 6 in the *Ttn3* locus is flanked with two *loxP* sites preceded by a FRT-flanked neo and lacZ cassettes.

(B) Representative traces of three types of MA currents in DRG neurons transfected with scrambled siRNA (Scrmbl) or *Ttn3*-siRNA (siRNA), or DRG neurons isolated from *Ttn3*$^{-/-}$ (KO) mice. The DRG neurons were stimulated by mechanical steps with 0.42 μm increments for 100 or 600 ms.

(C) Histogram of cell type among DRG neurons. DRG neurons were classified by inactivation kinetics of MA currents. Inactivation time constants (τ_i) for RA, IA, and SA MA currents were $\tau_i < 10$ ms, $10 < \tau_i < 30$ ms, and $\tau_i > 30$ ms, respectively.

(D) Distribution of the inactivation time constant (τ_i) of SA type MA currents in DRG neurons from control mice (solid circles) or isolated from *Ttn3* KO (open circles) mice.

potentials when the bath solution was changed to 150 mM NaCl, 150 mM KCl, 100 mM $CaCl_2$, or 100 mM $MgCl_2$, the permeability ratios (P_x/P_{cs}) between Na^+, K^+, Mg^{2+}, and Ca^{2+} and Cs^+ were 1.31 ± 0.04 (n = 9), 1.24 ± 0.05 (n = 6), 1.41 ± 0.15 (n = 6), and 2.01 ± 0.11 (n = 8), respectively (Figure 3F). Thus, TTN3 is a nonselective cationic channel with high permeability to Ca^{2+}.

Pharmacology of MA Currents

MA currents in DRG neurons are inhibited by gadolinium (Gd^{3+}) and other blockers (Drew et al., 2002, 2004; Drew and Wood, 2007; McCarter et al., 1999). To determine the pharmacological profile of TTN3, F11 cells transfected with *Ttn3* were stimulated by three consecutive mechanical stimuli of identical amplitude (4.2 or 4.6 μm). The TTN3 MA currents were reversibly inhibited by known mechanosensitive channel blockers. The application of 30 μM Gd^{3+}, which is a well-known MA channel blocker (Coste et al., 2010; McCarter et al., 1999), significantly inhibited the MA currents in TTN3-expressing cells (Figure 4A). The half-maximal concentration for inhibition (IC_{50}) of Gd^{3+} was 3.9 μM (n = 7–8) (Figure 4B). In addition, the TTN3 currents were markedly reduced by 30 μM ruthenium red or FM1-43, a fluorescent dye known to block MA currents in DRG neurons (Drew and Wood, 2007) (Figures 4A and 4C). More important, 2.5 μM GsMTx4, a purified tarantula toxin that inhibits MA currents in various cell types, also strongly inhibited the TTN3-mediated MA currents (Bae et al., 2011; Gottlieb et al., 2007) (Figures 4A and 4C). The TTN3-mediated MA currents were not blocked by 50 μM chloropromazine, a cup former membrane-modifying agent that is known to inhibit the MA TREK1 channel (Maingret et al., 2000), or by 10 μM HC030031, a TRPA1 blocker known to inhibit mechanosensitive currents (Kerstein et al., 2009). Modification of the property in TTN3-mediated MA currents by these chemicals or peptides also implies that TTN3 could be a major component of mechanosensitive ion channel.

Expression of TTN3 in DRG Neurons

A qPCR assay of three *Ttn* genes from 21 mouse tissues depicted a different expression pattern for each gene (Figure S3). TTN3 showed high expression in the epididymis, pancreas, DRG, eye, brain, and spinal cord. To observe the expression patterns of TTN3 in DRG, we generated anti-TTN3 antibody against a segment in the C terminus. This antibody appears to be specific, as it detected endogenous and overexpressed TTN3 but not in *Ttn3* siRNA transfected F11 cells (Figure 5A). Furthermore, when TTN3-IRES2-AcGFP was transfected in HEK293T cells, the immunofluorescence of TTN3 was detected in GFP-expressing cells (Figure 5B).

The immunofluorescence analysis of TTN3 in DRG neurons revealed unique expression pattern in DRG neuronal populations. About 61% (646 of 1,056 cells) of TTN3-positive cells were colocalized with neurofilament M, a marker for myelinated neurons (Figures 5C and 5E). In addition, 57% (499 of 878 cells) of TTN3-positive neurons were positive to parvalbumin, a marker for proprioceptive sensory neurons. TTN3-positive neurons were positive for nociceptor markers, TRPV1 (23%), or isolectin

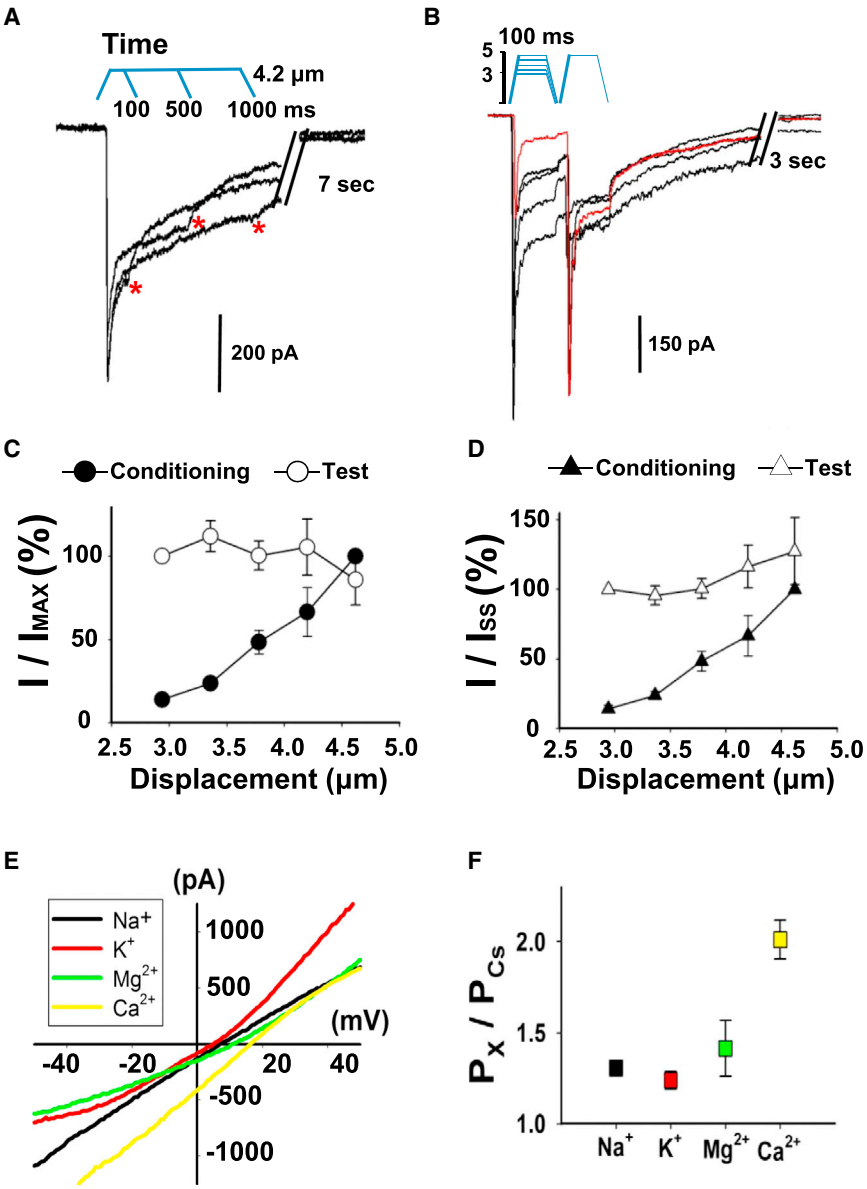

Figure 3. Biophysical Property of TTN3-Mediated MA Currents

(A) The steady-state current of a *Ttn3*-transfected F11 cell persisted up to 1 s for a prolonged mechanical step. Asterisks represent steady-state currents at the end of the mechanical stimuli.

(B) The effects of conditioning mechanical stimuli on MA currents of *Ttn3*-transfected cells. Conditioning mechanical stimuli of 100 ms duration with 2.9–4.6 μm indentations in 0.42 μm increments were applied, followed by a test step pulse with a 4.6 μm stimulus.

(C and D) Peak (C) and steady-state (D) currents induced by the conditioning and test mechanical steps. The peak or steady-state currents (I) were normalized with the maximal peak (I_{MAX}) or steady-state currents (I_{SS}). The steady-state currents were measured at the end of the mechanical steps (n = 4–5).

(E) Representative I-V relationships of steady-state MA currents obtained at different salt conditions in TTN3 overexpressing F11 cells. A voltage ramp (−80 to +80 mV) was applied within steady-state currents of TTN3 activation by mechanical stimuli. The pipette solution contained 150 mM CsCl. The bath solution contained 150 mM NaCl, 150 mM KCl, 100 mM $MgCl_2$, or 100 mM $CaCl_2$.

(F) Cation permeability ratios (P_X/P_{Cs}) of the steady-state MA currents in TTN3 expressing F11 cells (n = 6–9).

B4 (15%) (Figures 5C and 5E). We could not observe clear immunoreactivity in DRG neurons from *Ttn3* KO mice (Figure 5D).

Expression of TTN3 in MSs

Rich immunoreactivity of TTN3 was observed in MSs in extensor digitorum longus (EDL) muscles of mouse hindlimb (Figure 6A). The TTN3 immunoreactivity was prominent in the center region of MSs, where intrafusal muscle nuclei clustered (Barker, 1974; Bewick and Banks, 2015; Oliveira Fernandes and Tourtellotte, 2015; Tourtellotte and Milbrandt, 1998). In addition, TTN3 immunofluorescence was colocalized with neurofilament M in annulospiral structures wrapping round intrafusal muscles, typical primary afferents in MSs (Figures 6B and 6C) (Banks, 2015; de Nooij et al., 2015; Oliveira Fernandes and Tourtellotte, 2015). However, the TTN3 immunofluorescence was not observed in MSs of *Ttn3*-KO mice (Figure 6C).

The presence of TTN3 in MS prompted us to investigate the functional role of TTN3 in MS afferents by measuring MS afferent activities of wild-type (WT) and KO mice. Extracellular neural recording was made at the peroneal nerve attached to the isolated EDL muscle (de Nooij et al., 2015; Franco et al., 2014). Stretching the EDL muscles (~10 mm) isolated from WT mice by 2 mm for 5 s evoked a barrage of nerve discharges. However, the activity of the muscle stretch-evoked discharge in MS afferents from KO mice was dramatically reduced (Figures 6D and 6E). The reduction in spindle afferent activity was observed throughout the range of muscle stretch (1–3 mm) ($p < 0.0001$, two-way ANOVA, $F_{[1,\ 132]} = 56.5$). *Ttn3* KO mice showed a significant reduction in the sensitivity (slope) to muscle stretch compared with WT mice (5.81 ± 0.72 versus 2.77 ± 0.36 spikes/mm, $p < 0.001$, n = 23–24, Student's t test) (Figure 6E). These results indicate that TTN3 contributes to stretch-evoked MS afferent activity.

Loss of Motor Coordination in Ttn3 KO Mice

Because MS sensory input is essential for muscle coordination, behavior tests for determining muscle coordination were conducted. *Ttn3* KO mice spent less time clinging to an inverted grid compared with WT mice, a test for motor coordination and muscle strength because grip of the grid with all four limbs is

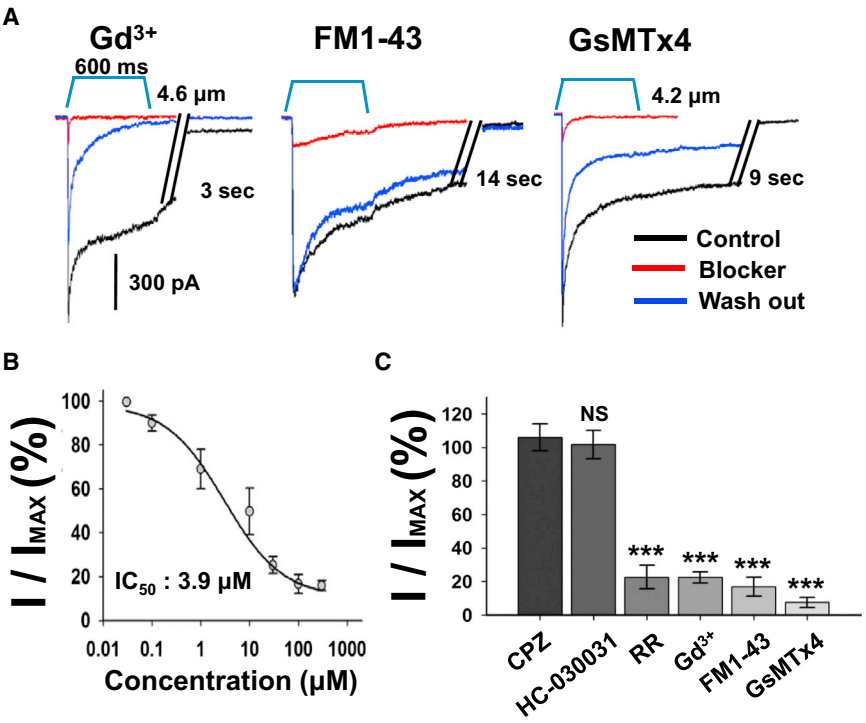

Figure 4. Pharmacological Profiles of TTN3-Mediated MA Currents

(A) Representative traces of TTN3-mediated MA currents in F11 cells after the application of 30 μM gadolinium (Gd^{3+}), 30 μM FM1-43, or 2.5 μM GsMTx4. Identical mechanical steps were repeated three times. Each blocker was applied for 1 min before the second mechanical step, followed by wash out for recovery.

(B) Dose-response relationship of Gd^{3+} in inhibiting the TTN3-mediated MA currents fitted to the Hill equation (IC_{50} = 3.9 μM, n = 7–8).

(C) The effects of 50 μM chloropromazine (CPZ), 10 μM HC-030031, 30 μM ruthenium red (RR), 30 μM Gd^{3+}, 30 μM FM1-43, and 2.5 μM GsMTx4 on the TTN3-mediated MA currents (n = 7–8). ***p < 0.001 compared with the I/I_{MAX} of CPZ treatment, one-way ANOVA, Tukey's post hoc test.

required for prolonged hanging (Cheret et al., 2013). Although WT mice continued to hang for longer than 10 min, the majority of KO mice fell within 2 min (Figure 7A). In a raised beam test (Bourane et al., 2015; Muller et al., 2008), KO mice made about three times more limb-slips and showed significantly slower time to cross the beam (4.6 s versus 6.5 s, $p < 0.01$, n = 10–11, Student's t test) than WT mice (Figure 7B). Furthermore, gait analysis with the CatWalk system revealed an abnormal gait in KO mice. The gait of KO mice showed significantly slower movement with reduced swing speed and stride length compared with WT mice (Figures 7C–7E). In addition, KO mice elicited reduced regularity index and phase dispersion in the fronto-hindlimb coordination (Figures 7F and 7G) (Dale et al., 2012; Encarnacion et al., 2011). In contrast, genetic ablation of *Ttn3* appeared not to affect general motor activity as well as tactile and pain sensation (Figure S4). These results support the idea that TTN3 regulates motor coordination through MS afferents in mouse.

DISCUSSION

Three types of MA currents, distinguished by their inactivation kinetics, are present in DRG neurons (Drew et al., 2002, 2004; Hao and Delmas, 2010; Hu and Lewin, 2006). The kinetically defined MA DRG neurons fire differently in response to sustained tactile stimuli. The RA neurons tend to fire brief phasic discharges, whereas the SA neurons elicit sustained discharges (Hao and Delmas, 2010). Piezo channels confer RA MA currents in many organs as well as DRG neurons. However, channel genes responsible for other kinetically defined currents in DRG neurons have not been identified. The present study provides evidence that TTN3 mediates SA currents in DRG neurons and presents typical biophysical and pharmacological profiles pertaining to SA mechanosensitive currents. Although there is a dramatic reduction in the number of SA-type neurons from *Ttn3*$^{-/-}$ mice, SA responses still remained in these mice. Thus, it is highly likely that there may be channels other than TTN3 that confer SA type currents.

Motor coordination is essential for survival, predation, and escape. Without proper motor coordination, elaborate movements cannot be carried out, because they require exact contraction timing of multiple flexor and extensor muscles. Motor coordination depends on proprioceptive sensory signals primarily from MS afferents in muscles (Proske and Gandevia, 2012; Proske et al., 2000; Rossi-Durand, 2006). Studies on genetic disruption of MS afferents supports the requirement of MS afferents for motor coordination (Cheret et al., 2013; Oliveira Fernandes and Tourtellotte, 2015; Tourtellotte and Milbrandt, 1998). During active muscle contraction or passive movements, MSs sense muscle stretch and report changes in length to the CNS (Banks, 1994; Ellaway et al., 2015). In the present study, TTN3 was expressed in MSs, and the genetic ablation of TTN3 led to a reduction in motor coordination. Thus, TTN3 appears to play a role in proprioception.

Skeletal muscle contains multiple MSs. The number of MSs varies in different muscles. In general, the density is high in muscles conducting fine movements, such as interrossei muscles in the hand, whereas its density is low in girdle muscles (Barker, 1974). MSs are found only in vertebrates in the animal kingdom (Barker, 1974). The structure of MS varies among vertebrates such that primitive forms of MSs were found in Amphibia (Barker, 1974). The presence of MSs in fish was controversial. Barker (1974) claimed that the fish does not have MSs (Barker, 1974). However, Maeda et al. (1983) found MSs in a jaw closing muscle in a Japanese salmon. Consistent with this, *Ttn* genes were found in all vertebrates, including chicken, turtle, frog, and zebrafish (Figure 1B).

A study of the ionic basis for receptor potential of MS afferents revealed that Na^+ and Ca^{2+} are responsible for the stretch-evoked receptor potential (Hunt et al., 1978). Thus, cationic

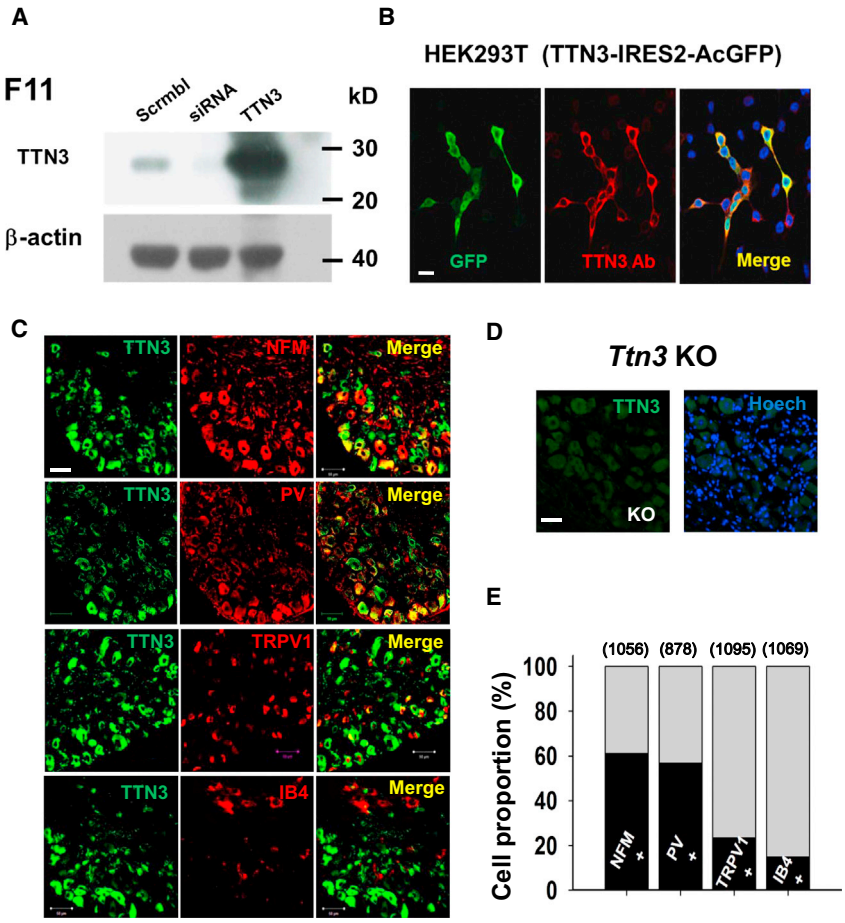

Figure 5. Expression of TTN3 in DRG Neurons

(A and B) Validation of TTN3 antibody. (A) Western blots with anti-TTN3 antibody in F11 cells. F11 cells were transfected with scrambled siRNA (scrmbl), *Ttn3* siRNA or TTN3-IRES2-AcGFP. (B) Immunofluorescent images in TTN3-IRES2-AcGFP transfected HEK293T cells stained with anti-TTN3 antibody. The scale bar represents 20 μm.

(C and D) Immunofluorescent images of TTN3 in WT (C) and KO (D) DRG neurons. The DRG neurons were stained with neurofilament M (NFM), parvalbumin (PV), TRPV1, and Isolectin B4 (IB4). The scale bar represents 50 μm.

(E) Percentages of NFM, PV, TRPV1, and IB4-positive neurons in the TTN3-positive DRG neurons. The numbers in parentheses represent the total number of TTN3-positive DRG neurons.

channels were considered to be candidate channels for mechanotransduction in MSs. Among them, ENaC was considered to be a candidate (Bewick and Banks, 2015). ENaC is a mammalian homolog of DEG channel found in *C. elegans*. ENaC is highly selective to Na^+ and blocked by amiloride (Garty and Palmer, 1997). ENaC immunoreactivity is found in MS afferents (Simon et al., 2010). Moreover, the activity of MS afferent is largely inhibited by amiloride application (Simon et al., 2010). These results suggest that ENaC appears to be a mechanotransduction channel in MS afferents. However, the mechanosensitivity of ENaC channel in mammals was controversial, because it is not activated by mechanical stimuli when expressed heterologously in mammalian cells (Awayda and Subramanyam, 1998; Drew et al., 2004). In addition, the loss-of-function phenotype for motor coordination has not been reported with ENaC-deficient mice. Recently, Piezo2 has been implicated in proprioception (Woo et al., 2015). Woo et al. (2015) found that Piezo2 is present in MSs, and its genetic deletion from muscle afferents leads to marked reduction in stretch-induced nerve activity of MS afferents as well as prominent loss of muscle coordination. Thus, Piezo2 is a major stretch-activated channel responsible for the ionic basis of MS afferents. Although the prominent phenotype of Piezo2-deficient mice undoubtedly stresses its roles in proprioception, this does not preclude the possible presence of other MA channels for proprioception. The inactivation kinetic of Piezo2 does not fit in the kinetics of MS afferent responses. Piezo2 inactivates rapidly after a brief activation, whereas most MS afferents respond as long as muscle stretch lasts. In addition, there would be a redundancy of genes in proprioception, which is also the case in other key physiological functions, such as heat sensation in the skin (Bandell and Patapoutian, 2012; Dhaka et al., 2006).

The function of the TMEM150/Tentonin genes is largely unknown except for a genetic link between TMEM150B/BRSK1 and menopause in women (He et al., 2009). Because of the low sequence similarity of TTN1 or TTN2 to TTN3, the function of TTN3 is unknown. Among these *Ttn* genes, only *Ttn3* responded well to mechanical stimuli. Although TTN3 can generate MA currents when expressed heterologously, the propensity of channel currents after transfection differs in cell types. Thus, whether it is activated by a direct stretch of the plasma membrane or with the help of tethering proteins remains to be clarified.

Because MS afferent function is essential for motor coordination, the identification of the mechanotransduction channel in MS afferents provides a route to dissecting the molecular mechanisms underlying motor coordination, which may be significant for understanding motor dysfunction in various human diseases. Identification of novel mechanosensitive ion channel will provide deeper understanding of uncovered various mechanosensations in mammals. Because TTN3 is expressed in nociceptors, we cannot rule out a possible role in nociception.

EXPERIMENTAL PROCEDURES

Molecular Cloning of the TTN Family

Primers were designed using the mouse cDNA sequences of *Ttn1-3 (Tmem150a-c)* from the NCBI database (Genbank: NM_144916.3, NM_177887, and NM_182841). Nucleotide fragments of 816, 717, and 750 for *Tmem150a-c* were amplified from cDNA libraries from the kidney, small intestine, and epididymis of adult C57BL/6J mice, respectively. Primers used for cloning are as follows: *Ttn1 (Tmem150a)* forward (5′-ctcgaggc caccatgaccgcct-3′) and *Ttn1* reverse (5′-aagcttgatcatggcaatactctcgggag-3′)

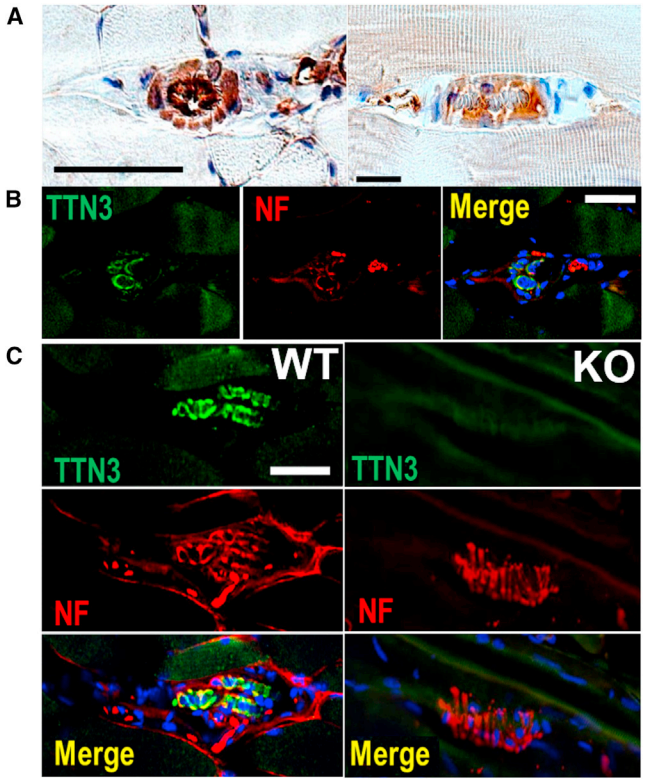

Figure 6. The Presence of TTN3 in MSs and the Reduction in Stretch-Evoked Muscle Afferent Activity in *Ttn3* KO Mice

(A) Immunohistochemistry of TTN3 in MSs of cross (left) and longitudinal (right) sections of EDL muscles. In cross section, heavy immunoreactivity of TTN3 was observed in intrafusal muscles. In longitudinal section, the TTN3 immunoreactivity surrounded nuclei of intrafusal muscles. H&E staining. Scale bars represent 20 μm.

(B and C) TTN3 immunofluorescence surrounding intrafusal muscles and annulospiral fibers in MSs of cross (B) and longitudinal (C) sections of EDL muscles from WT and *Ttn3* KO mice. Part of TTN3 is colocalized with neurofilament M (NF), a marker for myelinated nerve fibers. Nuclei were also stained in blue with Hoechst 33342.

(D) Stretch-evoked MS afferent activities of ex vivo muscle-nerve preparation of WT and KO mice. MS afferent activities were recorded with a suction electrode (70 μm in diameter)

(E) Summary of MS afferent activities of both genotypes in response to 1–3 mm stretches. ***$p < 0.001$, Student's t test.

with restriction sites for XhoI and HindIII, *Ttn2 (Tmem150b)* forward (5′-ctcgaggccaccatgtggaattacct-3′) and *Ttn2* reverse (5′-aagcttgagcacctgtgccatctgta-3′) with restriction sites for XhoI and KpnI, and *Ttn3 (Tmem150c)* forward (5′-ctcgaggccaccatggacgggaagaaat-3′) and *Ttn3* reverse (5′-ggtaccctcacctgatccgtctgatattc-3′) with restriction sites for XhoI and KpnI.

Ttn1-3 (tmem150a-c) fragments were cloned into pEGFP-N1 to have fusion proteins tagged with EGFP. The vector was mutated to include stop codons between the genes and the GFP sequence (pEGFP-N1[STOP]) to express the genes only. The genes were also sub-cloned into pIRES2-AcGFP1 to avoid the GFP fusion effects.

The protein sequence of mouse TTN1 (TMEM150a) is MTAWILLPVSLSAFSITGIWTVYAMAVMNRHVCPVENWSYNESCSPDPAEQGGPKSCCTLDDVPLISKCGTYPPESCLFSLIGNMGAVMVALICLLRYGQLLEQSRHSWINTTALITGCTNAAGLVVVGNFQVDHAKSLHYIGTGVAFTAGLLFVCLHCVLFYHGATTPLDMAMAYLRSVLAVIAFITLVLSGVFFLHESSQLQHGAALCEWVFVLDILIFYGTFSYEFGTISSDTLVAALQPAPGRACKSSGSSSTSTHLNCAPESIAMI.

The protein sequence of mouse TTN2 (TMEM150b) is MWNYLSLLPVILFLWAIAGIWIVFAIAVVNGSVDLNEGFPFISICGSYAPQSCIFGQVLNIGAALTVWICIVRHHQLRDWGVKTWQNQLILWSGILCALGTSIVGNFQDKNQKPTHLAGAFLAFILGNLYFWLQFFLSWWVKGLPQPGPHWIKSLRLSLCSLSTILIVAMIVLHALHMRSASAICEWVVAMLLFMLFGFFAVDFSILRGCTLHLHPRLDSSLPQAPSGSPNIQMAQVL.

The protein sequence of mouse TTN3 (TMEM150c) is MDGKKCSVWMFLPLVFTLFTSAGLWIVYFIAVEDDKILPLNSAARKSGAKHAPYISFAGDDPPASCVFSQVMNMAAFLALVVAVLRFIQLKPKVLNPWLNISGLAALCLASFGMTLLGNFQLTNDEEIHNVGTSLTFGFGTLTCWIQAALTLKVNIKNEGRRAGIPRVILSAVITLCVVLYFILMAQDIHMYAARVQWGLVMCFLAYFGTLAVEFRHYRYEIVCSEYQENFLSFSESLSEASEYQTDQV.

Cell Culture and Transfection

HEK293T and F11 cells were grown in DMEM (Life Technologies) supplemented with 10% fetal bovine serum (FBS), 2 mM L-glutamine, 1 mM sodium pyruvate, and 100 U/ml penicillin/streptomycin. Cells were plated on glass coverslips in DMEM supplemented with 10% FBS, 2 mM L-glutamine, and 100 U/mL penicillin/streptomycin in 35 mm dishes. The F11 cells were plated on laminin-coated (2 mg/mL) glass coverslips in DMEM supplemented with 1% FBS, 2 mM L-glutamine, and 100 U/mL penicillin/streptomycin in 35 mm dishes. Half of the medium was replaced every 2 days.

pIRES2-AcGFP1-TTN1, pIRES2-AcGFP1-TTN2, pIRES2-AcGFP1-TTN3, pEGFP-N1(STOP)-TTN1, pEGFP-N1(STOP)-TTN2, or pEGFP-N1(STOP)-TTN3 vector was transfected for 48 hr with Lipofectamine 2000 (Life Technologies) or FuGene (Promega). The pEGFP-N1 vector was used for transfection controls. The *Ttn3* and scrambled siRNA sets were designed, synthesized, and tagged with Cy3 fluorescence by the manufacturer (Bioneer). The siRNA was positioned at nucleotides 421–439. The sequence is *Tnt3*_siRNA sense 5′-GCUUGUGGAUAGUGUACUU (dTdT)-3′ and antisense 5′-CGAACTCCTATCACATGAA(dTdT)-3′. The Cy3-tagged siRNAs were applied to the cultured DRG cells using Lipofectamine 2000. The siRNA-treated cells were incubated for 48–72 hr before use.

Isolation of DRG Neurons

Primary cultures of DRG neurons were prepared as previously described (Cho et al., 2012). Briefly, thoracic and lumbar DRGs were dissected from 7- to 8-week-old mice and collected in ice-cold medium (DMEM/F12; Life Technologies). Isolated DRGs were then incubated in medium containing 2 mg/mL collagenase IA (Sigma) for 45 min at 37°C. Cells were washed three times with Ca^{2+}- and Mg^{2+}-free Hank's balanced salt solution (Life Technologies). The cells were washed gently two or three times with the culture medium, suspended, and gently triturated with a 1 mL pipette before plating onto round glass coverslips (Fisher). Cells were incubated in culture medium containing DMEM/F12, 10% FBS, 50 ng/mL nerve growth factor (Life Technologies), 5 ng/mL glial cell line-derived neurotrophic factor (Life Technologies), and 100 U/mL penicillin/streptomycin in 95% air/5% CO_2 atmosphere for 48–72 hr before use.

Channel Current Recording

Whole-cell currents were recorded using a voltage-clamp technique. Whole cells were formed by breaking the plasma membrane under a glass pipette after gigaseals were made. The resistance of the glass electrodes was 2–3 MΩ. The junctional potentials were adjusted to zero. The holding potential was set at −60 mV. Currents were amplified with Axopatch200B (Molecular Devices), filtered by 0.5 kHz, digitized at a sampling rate of 5 kHz with Digidata 1440 (Molecular Devices), and stored in a computer. The stored currents were later analyzed using pClamp software version 10.0 (Molecular Devices).

For DRG neuron recordings, the pipette solution contained 130 mM KCl, 2 mM $MgCl_2$, 5 mM EGTA, 10 mM HEPES, 2 mM Mg-ATP, 0.2 mM Na-GTP, and 20 mM D-mannitol. The pH of the solution was adjusted to 7.2 with KOH. The bath solution contained 130 mM NaCl, 5 mM KCl, 1 mM $CaCl_2$, 2 mM $MgCl_2$, 10 mM HEPES, and 10 mM D-mannitol at pH 7.2, adjusted with NaOH. For recording currents in cell lines, the pipette solution contained 130 mM CsCl, 2 mM $MgCl_2$, 10 mM HEPES, 2 mM Mg-ATP, 0.2 mM Na-GTP, and 25 mM D-mannitol. The pH was adjusted to 7.2 with CsOH. For the cation selectivity experiment, the pipette solution contained

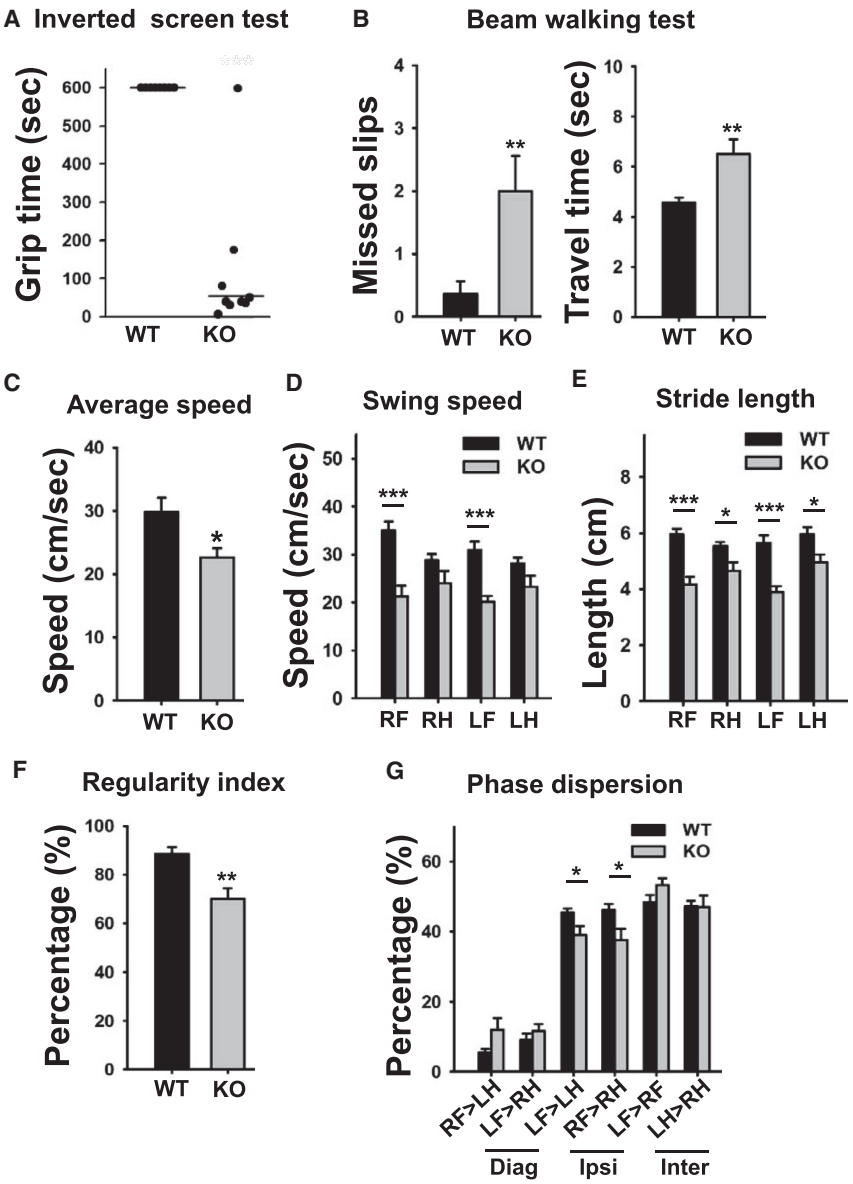

Figure 7. Loss of Motor Coordination in *Ttn3* KO Mice

(A) Inverted screen test. Mice were placed on an inverted grid screen. The duration of grip time of each mouse was measured. The cutoff time to cling to the inverted grid was 10 min. Horizontal bars represent average time to cling to the screen (n = 10–11). $p < 0.001$, Student's t test.

(B) Beam walking test. Mice were trained to walk on a 6 mm wide, 80 cm long beam. Their walk on the beam was video-recorded, and the number of missed slips and traveled time during walking were measured (n = 8–9). **$p < 0.01$, Student's t test.

(C–G) Gait analysis of mice with the CatWalk system. Mice walked on a glass floor on which their paw-prints were recorded. KO mice showed slower walking (C), reduced swing speed (D), and shorter stride length (E) than WT mice. KO mice also showed lower regularity index (F) in their walking patterns and different phase dispersion in fronto-hindlimb coordination (G) compared with WT mice. Diag, diagonal; Ipsi, ipsilateral; Inter, inter-limb; LF, left front paw; LH, left hind paw; RF, right front paw; RH, right hind paw (n = 8–10). *$p < 0.05$, **$p < 0.01$, ***$p < 0.001$, Student's t test.

150 mM CsCl and 10 mM HEPES at pH 7.2, adjusted with CsOH. The bath solution contained 150 mM NaCl, 150 mM KCl, 150 mM NMDG-Cl, 100 mM $CaCl_2$, or 100 mM $MgCl_2$ and 10 mM HEPES. The pH was adjusted to 7.2 with NaOH, KOH, or CsOH for divalent cation solutions. For the anion/cation permeability experiments, the pipette solution contained 70 mM NaCl, whereas the bath solution contained 210 mM NaCl. The osmolarity of all of the solutions was adjusted to 290 mOsm by adding D-mannitol. The P_{Cl}/P_{Na} of each mutant was obtained by measuring the reversal potential of the steady-state current of each mutant using the Goldman-Hodgkin-Katz equation (Arreola and Melvin, 2003).

To determine the current-voltage relationships, voltage ramps from −80 to +80 mV were applied for 150 ms to whole cells during 600 ms mechanical stimulation. For blocker experiments, 50 μM chloropromazine (Sigma), 10 μM HC-030031 (Sigma), 30 μM ruthenium red (Sigma), 30 μM FM1-43 (Biotium), 2.5 μM GsMTx-4 (Tocris), or 30 μM $GdCl_3$ (Sigma) was added to the bath solution. To get a dose-response curve for the Gd^{3+} inhibition, the normalized current (I/I_{MAX}) was fitted to the Hill equation, I/I_{MAX} (%) = $[1 + (K_D/[Gd^{3+}])^n]^{-1}$, where K_D represents the half-maximal effect of Gd^{3+} and n is the Hill coefficient.

Mechanical Stimulation

A fire-polished glass electrode (tip diameter ~ 3–4 μm) was positioned at an angle of ~50° to the cell surface. The probe was moved by a micromanipulator (Nano-controller NC4; Kleindiek Nanotechnik). The movement of the probe was controlled either by a joystick or by a computer. The initial position of the probe on the cell surface was determined by looking at the indentation of the cell surface through a microscope. Then, 1.0 μm retraction was made, which was considered to be the initial point of all mechanical stimuli. From the initial position, the mechanical steps were made by moving the glass probe forward from 2.5–7.2 μm in 0.42 μm increments. The typical duration of the mechanical stimulation was 100 or 600 ms.

Recording of MS Afferent Activity

The muscle-nerve ex vivo preparation and recording muscle fiber activity were described by others (Franco et al., 2014; Wilkinson et al., 2012). Briefly, mice were deeply anesthetized with isoflurane, decapitated immediately, and skinned. EDL muscle and the peroneal nerve attached to it were isolated in the chilled (4°C) solution containing 128 mM NaCl, 1.9 mM KCl, 1.2 mM KH_2PO_4, 26 mM $NaHCO_3$, 0.85 mM $CaCl_2$, 6.5 mM $MgSO_4$, and 10 mM glucose (pH 7.4). The isolated EDL muscle-nerve preparation was mounted into a tissue bath filled with the oxygenated solution containing 123 mM NaCl, 3.5 mM KCl, 0.7 mM $MgSO_4$, 1.7 mM NaH_2PO_4, 2.0 mM $CaCl_2$, 9.5 mM $NaC_6H_{11}O$, 5.5 mM glucose, 7.5 mM sucrose, and 10 HEPES (pH 7.4). Thin silk sutures were used to tie both ends of the EDL muscle to a micrometer and a force transducer for adjusting muscle stretch and measuring force. The output signal of the force transducer was amplified to report the magnitude of muscle stretch, which was well correlated with force applied to the muscles. A suction electrode was made with a glass pipette whose tip diameter was 70 μm. The suction electrode was filled with the bath solution. The free end of the peroneal nerve was suctioned into the electrode. To identify MS afferents, suctions were repeated until neuronal activities were observed during muscle stretches. Stretches for 5 s in length of 2 mm were repeated three times and two more stretches with stretch

lengths of 1 and 3 mm. Electrical signals in the suction electrode were amplified with ISO-80 (World Precision Instruments), filtered by 1 kHz, digitized at a sampling rate of 10 kHz with Digidata 1322 (Molecular Devices), and stored in a computer. The stored traces were later analyzed using the pClamp software version 10.0. Spikes above 1 SD of the noise were counted as action potentials of the nerve.

Phylogenetic Analysis

Multiple sequence alignments and the phylogenetic dendrogram were performed using the CLUSTALW program. GenBank accession numbers are shown in Table S1.

Antibody Production

A peptide spanning the C terminus of mouse TTN3 (211–249 amino acids: LAVEFRHYRYEIVCSEYQENFLSFSESLSEASEYQTDQV) was synthesized and immunized three times to a rabbit (AbFrontier). The immunized rabbit serum was purified with protein A-Sepharose column chromatography and with antigen-specific affinity column. The specificity of purified antibody was confirmed by ELISA.

Animals and *Ttn3* KO Mice

Mice were used under protocols approved by the Institute of Laboratory Animal Resources of the Seoul National University. Typically, 7- to 8-week-old mice were used for all experiments.

The mutant mouse was generated by the trans-National Institutes of Health Mouse Initiative Knockout Mouse Project (https://www.komp.org). Briefly, *LacZ* was inserted between exons 5 and 6 of the *Ttn3* locus with stop codon, which resulted in the expression of truncated *Ttn3* and *LacZ* fusion protein. The $Ttn3^{+/-}$ mice were crossed with WT mouse to produce additional $Ttn3^{+/-}$ mice. These $Ttn3^{+/-}$ mice were then crossed each other to further produce $Ttn3^{-/-}$ mice.

Immunohistochemistry

Mouse EDL muscles were fixed in 4% paraformaldehyde for 24 hr, paraffin embedded, and cut in 5 μm sections with a vibratome. Each section was incubated with 3% H_2O_2 in methanol for 30 min to quench endogenous peroxidase activity. Tissue sections were dehydrated with graded alcohols and exposed to 10 mM sodium citrate for antigen retrieval. The sections were blocked with PBS containing 5% normal goat serum and 0.3% Triton X-100 for 1 hr at room temperature and then incubated with anti-TTN3 (1:100) antibody diluted in PBS containing 1% BSA and 0.3% Triton X-100 overnight at 4°C. The sections were subsequently washed three times, incubated for 1 hr with HRP-conjugated secondary antibody, incubated with 3,3′-diaminobenzidine tetrahydrochloride (Sigma) after wash, and immediately washed under tap water after the color development. Slides were stained with H&E.

Immunofluorescence

Immunofluorescent staining of tissue sections was performed as previously described (Cho et al., 2012). Briefly, DRGs or EDL muscles were isolated from adult mice (7–8 weeks) and sectioned on a cryostat at 10 μm and fixed in 4% paraformaldehyde. Sections were washed and incubated with blocking buffer (10% goat serum or 4% BSA in PBS with 0.1% Triton-X) for 1 hr. Polyclonal TTN3 (1:700), TRPV1 (AB5566, Millipore, 1:500), or NFM (sc-51683, Santa Cruz, 1:500) antibody was incubated with samples in the blocking buffer overnight at 4°C or 48 hr at 4°C for muscles. Samples were then washed and incubated with Alexa Fluor 546-conjugated goat anti-rabbit (A11010, Life Technology, 1:500), Alexa Fluor 488-conjugated goat anti-guinea pig (AP193F, Invitrogen, 1:800), Alexa Fluor 488-conjugated goat anti-chicken (A11039, Invitrogen, 1:800), or isolectin B4 (I21411, Invitrogen, 20 μg/mL) at room temperature for 1 hr. Nucleus was stained using Hoechst 33342 for 10 min (H3570, Thermofisher Scientific, 1:2,000) The sections were imaged with a confocal microscope (LSM700; Carl Zeiss).

Western Blot

Mammalian Protein Extraction Reagent (Thermo) and a complete protease inhibitor cocktail (Roche) were added to F11 cell cultures to lyse cells. Lysates were then scraped off and centrifuged at 13,000 rpm for 10 min to obtain the supernatant of cell extracts. The supernatant was then denatured at 100°C and separated on a 4%–12% NuPAGE Bis-Tris gel (Invitrogen) and transferred onto polyvinylidene difluoride membranes. After blocking with 5% skim milk, the membranes were incubated with TTN3 (1:1,000) or β-actin (1:5,000, Sigma, A2066) antibody overnight at 4°C. The membranes were washed three times with Tris-buffered saline supplemented with 0.05% Tween 20. The membranes were incubated with anti-rabbit IgG-horseradish peroxidase secondary antibody (1:2,000, Cell Signaling, 7074S). The bands were visualized using the enhanced chemiluminescence reagent (Pierce).

Inverted Screen Test

Mice are allowed to grip a welded wire mesh (560 × 510 mm) composed of small squares (11.5 × 11.5 mm, 0.8 mm in diameter) with their all paws (Cassani et al., 2015; Jeyakumar et al., 1999). The mesh was then slowly inverted and held steadily 30 cm above a soft surface. Hanging time was measured until mice fell down. The cutoff time was set at 600 s.

Beam Walking Test

The beam walking test for WT and Ttn3 KO mice was performed as described elsewhere (Carter et al., 2001; Chort et al., 2013; Yokoi et al., 2012). Briefly, mice were trained to travel a 12-mm-wide plastic beam (80 cm long, 50 cm high) three times a day for 2 days, followed by 6-mm-wide beam three times. At the end of the bar, there was a dark cage so that mice were allowed to cross the beam to hide themselves. On the third day, mice were allowed to travel the 6-mm-wide beam. Movements of mice were recorded by video. Traveling time and the number of foot slips were measured.

CatWalk Gait Analysis

Mouse gait was analyzed as described elsewhere (Côté et al., 2012; Encarnacion et al., 2011; Hamers et al., 2006; Lucas et al., 2015). Briefly, gait analysis was assessed using the CatWalk system (Noldus Information Technology). The apparatus was consisted of a 1.3 m long glass floor under which a light source illuminated the floor in a dark environment. When a mouse was walking through the floor, the plantar regions of the mouse's paws glowed because of the light deflection. The footprints were then recorded by a video camera and stored in a computer. Mice were subjected to three successive runs. A mouse run was considered successful if a mouse walked the walkway in 5 s. After identification and labeling of each footprint, gait parameters were analyzed with CatWalk XT software. All parameters of each mouse represented averages of three trials. Average speed is the velocity of a mouse. Swing speed is the velocity of the moving limb during the swing phase. Stride length is the length of the stride cycle. Regularity index is the percentage of normal step-sequence patterns relative to the total number of paw placements. Phase dispersion is the percentage of initial contact of one paw (target paw) relative to the stride cycle of another paw (anchor paw).

Statistical Analysis

Data in the figures are shown as mean ± SEM. To compare two means, unpaired two-tailed Student's t tests were used. One-way or two-way ANOVA was used to compare multiple means.

SUPPLEMENTAL INFORMATION

Supplemental Information incudes Supplemental Experimental Procedures, four figures, one table, and one movie and can be found with this article online at http://dx.doi.org/10.1016/j.neuron.2016.05.029.

AUTHOR CONTRIBUTIONS

G.-S.H. cloned TTN3 and determined the biophysical property of TTN3. B.L. maintained KO mice and performed behavioral studies. J.W. and H.C. helped with molecular analysis. H.K., J.J., and J.Y.C. worked on bioinformatics. T.-R.R., G.H.K., and I.-B.K. worked on immunostaining. U.O. conceptualized and designed experiments and wrote the manuscript.

ACKNOWLEDGMENTS

We thank Prof. John N. Wood, FRS, University College London, for his critical comments on the manuscript. We also thank Prof. Myoung-Hwan Kim, Department of Physiology, Seoul National University, for his technical assistance. This study was supported by the National Research Foundation of Korea, funded by the Ministry of Science, ICT and Future Planning (2011-0018358) and by the BK21+ program of the Ministry of Education of Korea.

Received: December 20, 2015
Revised: April 2, 2016
Accepted: May 16, 2016
Published: June 16, 2016

REFERENCES

Akay, T., Tourtellotte, W.G., Arber, S., and Jessell, T.M. (2014). Degradation of mouse locomotor pattern in the absence of proprioceptive sensory feedback. Proc. Natl. Acad. Sci. U S A *111*, 16877–16882.

Arreola, J., and Melvin, J.E. (2003). A novel chloride conductance activated by extracellular ATP in mouse parotid acinar cells. J. Physiol. *547*, 197–208.

Awayda, M.S., and Subramanyam, M. (1998). Regulation of the epithelial Na+ channel by membrane tension. J. Gen. Physiol. *112*, 97–111.

Bae, C., Sachs, F., and Gottlieb, P.A. (2011). The mechanosensitive ion channel Piezo1 is inhibited by the peptide GsMTx4. Biochemistry *50*, 6295–6300.

Bandell, M., and Patapoutian, A. (2012). A hot new channel. Nat. Neurosci. *15*, 931–933.

Banks, R.W. (1994). The motor innervation of mammalian muscle spindles. Prog. Neurobiol. *43*, 323–362.

Banks, R.W. (2015). The innervation of the muscle spindle: a personal history. J. Anat. *227*, 115–135.

Barker, D. (1974). The morphology of muscle receptors. In Muscle Receptors, C.C. Hunt, ed. (Springer-Verlag), pp. 1–190.

Bewick, G.S., and Banks, R.W. (2015). Mechanotransduction in the muscle spindle. Pflugers Arch. *467*, 175–190.

Bourane, S., Grossmann, K.S., Britz, O., Dalet, A., Del Barrio, M.G., Stam, F.J., Garcia-Campmany, L., Koch, S., and Goulding, M. (2015). Identification of a spinal circuit for light touch and fine motor control. Cell *160*, 503–515.

Carter, R.J., Morton, J., and Dunnett, S.B. (2001). Motor coordination and balance in rodents. Curr. Protoc. Neurosci. *Chapter 8*, Unit 8.12.

Cassani, J., Ferreyra-Cruz, O.A., Dorantes-Barrón, A.M., Villaseñor, R.M., Arrieta-Baez, D., and Estrada-Reyes, R. (2015). Antidepressant-like and toxicological effects of a standardized aqueous extract of Chrysactinia mexicana A. Gray (Asteraceae) in mice. J. Ethnopharmacol. *171*, 295–306.

Chalfie, M. (2009). Neurosensory mechanotransduction. Nat. Rev. Mol. Cell Biol. *10*, 44–52.

Cheret, C., Willem, M., Fricker, F.R., Wende, H., Wulf-Goldenberg, A., Tahirovic, S., Nave, K.A., Saftig, P., Haass, C., Garratt, A.N., et al. (2013). Bace1 and Neuregulin-1 cooperate to control formation and maintenance of muscle spindles. EMBO J. *32*, 2015–2028.

Cho, H., Yang, Y.D., Lee, J., Lee, B., Kim, T., Jang, Y., Back, S.K., Na, H.S., Harfe, B.D., Wang, F., et al. (2012). The calcium-activated chloride channel anoctamin 1 acts as a heat sensor in nociceptive neurons. Nat. Neurosci. *15*, 1015–1021.

Chort, A., Alves, S., Marinello, M., Dufresnois, B., Dornbierer, J.G., Tesson, C., Latouche, M., Baker, D.P., Barkats, M., El Hachimi, K.H., et al. (2013). Interferon β induces clearance of mutant ataxin 7 and improves locomotion in SCA7 knock-in mice. Brain *136*, 1732–1745.

Coste, B., Mathur, J., Schmidt, M., Earley, T.J., Ranade, S., Petrus, M.J., Dubin, A.E., and Patapoutian, A. (2010). Piezo1 and Piezo2 are essential components of distinct mechanically activated cation channels. Science *330*, 55–60.

Côté, M.P., Detloff, M.R., Wade, R.E., Jr., Lemay, M.A., and Houlé, J.D. (2012). Plasticity in ascending long propriospinal and descending supraspinal pathways in chronic cervical spinal cord injured rats. Front. Physiol. *3*, 330.

Dale, J.M., Villalon, E., Shannon, S.G., Barry, D.M., Markey, R.M., Garcia, V.B., and Garcia, M.L. (2012). Expressing hNF-LE397K results in abnormal gaiting in a transgenic model of CMT2E. Genes Brain Behav. *11*, 360–365.

de Nooij, J.C., Simon, C.M., Simon, A., Doobar, S., Steel, K.P., Banks, R.W., Mentis, G.Z., Bewick, G.S., and Jessell, T.M. (2015). The PDZ-domain protein Whirlin facilitates mechanosensory signaling in mammalian proprioceptors. J. Neurosci. *35*, 3073–3084.

Delmas, P., and Coste, B. (2013). Mechano-gated ion channels in sensory systems. Cell *155*, 278–284.

Dhaka, A., Viswanath, V., and Patapoutian, A. (2006). Trp ion channels and temperature sensation. Annu. Rev. Neurosci. *29*, 135–161.

Drew, L.J., and Wood, J.N. (2007). FM1-43 is a permeant blocker of mechanosensitive ion channels in sensory neurons and inhibits behavioural responses to mechanical stimuli. Mol. Pain *3*, 1.

Drew, L.J., Wood, J.N., and Cesare, P. (2002). Distinct mechanosensitive properties of capsaicin-sensitive and -insensitive sensory neurons. J. Neurosci. *22*, RC228.

Drew, L.J., Rohrer, D.K., Price, M.P., Blaver, K.E., Cockayne, D.A., Cesare, P., and Wood, J.N. (2004). Acid-sensing ion channels ASIC2 and ASIC3 do not contribute to mechanically activated currents in mammalian sensory neurones. J. Physiol. *556*, 691–710.

Ellaway, P.H., Taylor, A., and Durbaba, R. (2015). Muscle spindle and fusimotor activity in locomotion. J. Anat. *227*, 157–166.

Encarnacion, A., Horie, N., Keren-Gill, H., Bliss, T.M., Steinberg, G.K., and Shamloo, M. (2011). Long-term behavioral assessment of function in an experimental model for ischemic stroke. J. Neurosci. Methods *196*, 247–257.

Franco, J.A., Kloefkorn, H.E., Hochman, S., and Wilkinson, K.A. (2014). An in vitro adult mouse muscle-nerve preparation for studying the firing properties of muscle afferents. J. Vis. Exp. *91*, 51948.

Garty, H., and Palmer, L.G. (1997). Epithelial sodium channels: function, structure, and regulation. Physiol. Rev. *77*, 359–396.

Ghil, S.H., Kim, B.J., Lee, Y.D., and Suh-Kim, H. (2000). Neurite outgrowth induced by cyclic AMP can be modulated by the alpha subunit of Go. J. Neurochem. *74*, 151–158.

Gottlieb, P.A., Suchyna, T.M., and Sachs, F. (2007). Properties and mechanism of the mechanosensitive ion channel inhibitor GsMTx4, a therapeutic peptide derived from tarantula venom. Curr. Top. Membr. *59*, 81–109.

Hamers, F.P., Koopmans, G.C., and Joosten, E.A. (2006). CatWalk-assisted gait analysis in the assessment of spinal cord injury. J. Neurotrauma *23*, 537–548.

Hao, J., and Delmas, P. (2010). Multiple desensitization mechanisms of mechanotransducer channels shape firing of mechanosensory neurons. J. Neurosci. *30*, 13384–13395.

He, C., Kraft, P., Chen, C., Buring, J.E., Paré, G., Hankinson, S.E., Chanock, S.J., Ridker, P.M., Hunter, D.J., and Chasman, D.I. (2009). Genome-wide association studies identify loci associated with age at menarche and age at natural menopause. Nat. Genet. *41*, 724–728.

Hu, J., and Lewin, G.R. (2006). Mechanosensitive currents in the neurites of cultured mouse sensory neurones. J. Physiol. *577*, 815–828.

Huang, M., and Chalfie, M. (1994). Gene interactions affecting mechanosensory transduction in Caenorhabditis elegans. Nature *367*, 467–470.

Hunt, C.C. (1974). The physiology of muscle receptors. In Muscle Receptors, C.C. Hunt, ed. (Springer-Verlag), pp. 191–234.

Hunt, C.C., and Ottoson, D. (1975). Impulse activity and receptor potential of primary and secondary endings of isolated mammalian muscle spindles. J. Physiol. *252*, 259–281.

Hunt, C.C., Wilkinson, R.S., and Fukami, Y. (1978). Ionic basis of the receptor potential in primary endings of mammalian muscle spindles. J. Gen. Physiol. *71*, 683–698.

Ikeda, R., Cha, M., Ling, J., Jia, Z., Coyle, D., and Gu, J.G. (2014). Merkel cells transduce and encode tactile stimuli to drive Aβ-afferent impulses. Cell *157*, 664–675.

Jeyakumar, M., Butters, T.D., Cortina-Borja, M., Hunnam, V., Proia, R.L., Perry, V.H., Dwek, R.A., and Platt, F.M. (1999). Delayed symptom onset and increased life expectancy in Sandhoff disease mice treated with N-butyldeoxynojirimycin. Proc. Natl. Acad. Sci. U S A *96*, 6388–6393.

Kerstein, P.C., del Camino, D., Moran, M.M., and Stucky, C.L. (2009). Pharmacological blockade of TRPA1 inhibits mechanical firing in nociceptors. Mol. Pain *5*, 19.

Levina, N., Tötemeyer, S., Stokes, N.R., Louis, P., Jones, M.A., and Booth, I.R. (1999). Protection of Escherichia coli cells against extreme turgor by activation of MscS and MscL mechanosensitive channels: identification of genes required for MscS activity. EMBO J. *18*, 1730–1737.

Li, J., Hou, B., Tumova, S., Muraki, K., Bruns, A., Ludlow, M.J., Sedo, A., Hyman, A.J., McKeown, L., Young, R.S., et al. (2014). Piezo1 integration of vascular architecture with physiological force. Nature *515*, 279–282.

Lucas, E.K., Reid, C.S., McMeekin, L.J., Dougherty, S.E., Floyd, C.L., and Cowell, R.M. (2015). Cerebellar transcriptional alterations with Purkinje cell dysfunction and loss in mice lacking PGC-1α. Front. Cell. Neurosci. *8*, 441.

Maeda, N., Miyoshi, S., and Toh, H. (1983). First observation of a muscle spindle in fish. Nature *302*, 61–62.

Maingret, F., Patel, A.J., Lesage, F., Lazdunski, M., and Honoré, E. (2000). Lysophospholipids open the two-pore domain mechano-gated K(+) channels TREK-1 and TRAAK. J. Biol. Chem. *275*, 10128–10133.

McCarter, G.C., Reichling, D.B., and Levine, J.D. (1999). Mechanical transduction by rat dorsal root ganglion neurons in vitro. Neurosci. Lett. *273*, 179–182.

Muller, K.A., Ryals, J.M., Feldman, E.L., and Wright, D.E. (2008). Abnormal muscle spindle innervation and large-fiber neuropathy in diabetic mice. Diabetes *57*, 1693–1701.

O'Hagan, R., Chalfie, M., and Goodman, M.B. (2005). The MEC-4 DEG/ENaC channel of Caenorhabditis elegans touch receptor neurons transduces mechanical signals. Nat. Neurosci. *8*, 43–50.

Oliveira Fernandes, M., and Tourtellotte, W.G. (2015). Egr3-dependent muscle spindle stretch receptor intrafusal muscle fiber differentiation and fusimotor innervation homeostasis. J. Neurosci. *35*, 5566–5578.

Proske, U., and Gandevia, S.C. (2012). The proprioceptive senses: their roles in signaling body shape, body position and movement, and muscle force. Physiol. Rev. *92*, 1651–1697.

Proske, U., Wise, A.K., and Gregory, J.E. (2000). The role of muscle receptors in the detection of movements. Prog. Neurobiol. *60*, 85–96.

Ranade, S.S., Qiu, Z., Woo, S.H., Hur, S.S., Murthy, S.E., Cahalan, S.M., Xu, J., Mathur, J., Bandell, M., Coste, B., et al. (2014a). Piezo1, a mechanically activated ion channel, is required for vascular development in mice. Proc. Natl. Acad. Sci. U S A *111*, 10347–10352.

Ranade, S.S., Woo, S.H., Dubin, A.E., Moshourab, R.A., Wetzel, C., Petrus, M., Mathur, J., Bégay, V., Coste, B., Mainquist, J., et al. (2014b). Piezo2 is the major transducer of mechanical forces for touch sensation in mice. Nature *516*, 121–125.

Rossi-Durand, C. (2006). Proprioception and myoclonus. Neurophysiol. Clin. *36*, 299–308.

Simon, A., Shenton, F., Hunter, I., Banks, R.W., and Bewick, G.S. (2010). Amiloride-sensitive channels are a major contributor to mechanotransduction in mammalian muscle spindles. J. Physiol. *588*, 171–185.

Sukharev, S.I., Blount, P., Martinac, B., Blattner, F.R., and Kung, C. (1994). A large-conductance mechanosensitive channel in E. coli encoded by mscL alone. Nature *368*, 265–268.

Tourtellotte, W.G., and Milbrandt, J. (1998). Sensory ataxia and muscle spindle agenesis in mice lacking the transcription factor Egr3. Nat. Genet. *20*, 87–91.

Walker, R.G., Willingham, A.T., and Zuker, C.S. (2000). A Drosophila mechanosensory transduction channel. Science *287*, 2229–2234.

Wilkinson, K.A., Kloefkorn, H.E., and Hochman, S. (2012). Characterization of muscle spindle afferents in the adult mouse using an in vitro muscle-nerve preparation. PLoS ONE *7*, e39140.

Woo, S.H., Ranade, S., Weyer, A.D., Dubin, A.E., Baba, Y., Qiu, Z., Petrus, M., Miyamoto, T., Reddy, K., Lumpkin, E.A., et al. (2014). Piezo2 is required for Merkel-cell mechanotransduction. Nature *509*, 622–626.

Woo, S.H., Lukacs, V., de Nooij, J.C., Zaytseva, D., Criddle, C.R., Francisco, A., Jessell, T.M., Wilkinson, K.A., and Patapoutian, A. (2015). Piezo2 is the principal mechanotransduction channel for proprioception. Nat. Neurosci. *18*, 1756–1762.

Yang, Y.D., Cho, H., Koo, J.Y., Tak, M.H., Cho, Y., Shim, W.S., Park, S.P., Lee, J., Lee, B., Kim, B.M., et al. (2008). TMEM16A confers receptor-activated calcium-dependent chloride conductance. Nature *455*, 1210–1215.

Yokoi, F., Dang, M.T., Yang, G., Li, J., Doroodchi, A., Zhou, T., and Li, Y. (2012). Abnormal nuclear envelope in the cerebellar Purkinje cells and impaired motor learning in DYT11 myoclonus-dystonia mouse models. Behav. Brain Res. *227*, 12–20.

Neuron, Volume *91*

Supplemental Information

Tentonin 3/TMEM150c Confers Distinct Mechanosensitive Currents in Dorsal-Root Ganglion Neurons with Proprioceptive Function

Gyu-Sang Hong, Byeongjun Lee, Jungwon Wee, Hyeyeon Chun, Hyungsup Kim, Jooyoung Jung, Joo Young Cha, Tae-Ryong Riew, Gyu Hyun Kim, In-Beom Kim, and Uhtaek Oh

SUPPLEMENTAL FIGURES

Supplemental Figure Legends

Figure S1. The localization of TTN3 in the plasma membrane when overexpressed in HEK293T and F11 cells. (Related to Figure 1)

A fusion protein, TTN3-GFP was overexpressed in HEK293T or F11 cells and stained with Hoechst 33342. GFP alone was also overexpressed in HEK293T cells for comparison (right panel).

Figure S2. Activation of TTN3 by mechanical step stimuli when transfected to HeLa cells. (Related to Figure 1)

(A) Representative traces of the currents activated by mechanical steps in *Ttn3*- and *Gfp*-transfected HeLa cells. After forming a whole cell, mechanical steps of 600 ms duration were applied to the surface. E_{hold} = -60 mV.

(B) Average peak amplitudes of MA currents activated by a 5.0 μm mechanical step in *Ttn3*- (grey), and *Gfp*-transfected (black) HeLa cells. Bars represent S.E.M. The numbers in brackets represent the number of cells tested. ***p < 0.001, Student's *t*-test.

Figure S3. Expression profiles of *Ttn* genes (Related to Figure 5).

Quantitative PCR was conducted from 21 adult mouse organs. The expression levels were normalized to the mRNA level of GAPDH. Bars represent the average of three experiments.

Figure S4. Behavioral tests for tactile, vibration or pain sensation and locomotor activity in *Ttn*3 KO mice (Related to Figure 7).

(A) Withdrawal percentage of WT (●) and KO (▲) mice to von Frey hair stimuli. Both hind paws were stimulated with von Frey hairs. Withdrawal percentage was determined by the proportion of responses to four stimulations with each hair. (n = 9 each genotype).

(B) The withdrawal latency of WT and KO mice to thermal stimuli in Hargreaves test. Radiant heat stimulus (IR = 50) was applied to left hind paws. Numbers in the bracket represent the number of experimental animals.

(C) Vibration preference test. Mice were placed in a chamber where two plates, one vibrating and non-vibrating plates were housed. Mice were allowed to wander around freely for 10 min. Time spent on each plate was measured from recorded video. The percentage of time represents the time spent on each plate divided by total time spent in the chamber.

(D) Total distance of mice moved in an open field. The movement of a mouse was measured for 40 min.

Table S1. Phylogenetic Analysis (Related to experimental procedures)

GenBank accession IDs are shown.

Supplementary Information Video (Related to Figure 1)

The video shows the whole-cell current recording of a HEK293T cell transfected with *Ttn3*. The movie clip of the cell stimulated by a stimulus glass probe (on the left) with a recording glass pipette (on the right) was superimposed with the current trace.

SUPPLEMENTAL EXPERIMENTAL PROCEDURE

Real time quantitative PCR

All tissues were freshly isolated from adult C57BL/6J mice. The total RNA samples were extracted using the Total RNA Extraction Kit (Intron). The first strand cDNA was synthesized using the GoScript reverse transcription kit (Promega). The templates were amplified using Power SYBR Green PCR Master Mix (Applied Biosystems). Experiments were carried out in duplicate using the ABI StepOne Plus and StepOne real-time system. The product calibrations and normalizations were performed using the 2-Δcycle threshold (Ct) method (Schmittgen and Livak, 2008), where ΔCt = (Ct (target gene) - Ct (reference gene)). For the analysis of mRNA expression in different tissues, GAPDH was used as a reference gene. The following primer pairs were used.

Ttn1: 5′-ggtcctacaatgaatcctgctc-3′ (forward),

5′-ggccaccataacagcaccc-3′ (reverse)

Ttn2: 5′-tgtcctggtgggtgaaagg-3′ (forward),

5′-tcatagccacgatgaggatgg-3′ (reverse)

Ttn3: 5′-cgtgtggatgtttctacctctc-3′ (forward),

5′-gcacccgatttccttgcag-3′ (reverse)

GAPDH: 5′-aggtcggtgtgaacggatttg-3′ (forward),

5′-tgtagaccatgtagttgaggtca-3′ (reverse).

von Frey test

This test was performed using calibrated von Frey filaments (Stoelting Co., Wood Dale, IL) by poking the plantar region of the hindpaw. Mouse was placed in a transparent acrylic box with a mesh grid floor and adapted for 1 hour before the experiment. Plantar region of the hindpaw was poked with von Frey filaments with different thickness. Withdrawal percentage was determined by the proportion of withdrawal responses out of 4 stimulations.

Hargreaves test

This test was performed using a standard apparatus (Ugo Basile Biological research Apparatus). Briefly, a mouse was placed in a transparent acrylic box and adapted for 1 hour before the experiment. A radiant stimulus (intensity 50) was applied to the plantar surface of targeted hindpaw using infrared heat lamp. Each test was repeated three times in 5-min interval. The paw withdrawal latency of each mouse was the average of the three measurements.

Open field test

This test was performed using the Auto-Track system (Columbus Instruments). Mice were placed in a 37 × 37 cm activity cage. The animal movements were detected in the horizontal and vertical planes of optical tracking frame. Distance moved indicates the total distance of movement during 40 min in the activity cage.

References

Schmittgen, T.D., and Livak, K.J. (2008). Analyzing real-time PCR data by the comparative C(T) method. Nat Protoc 3, 1101-1108.

Figure S1.

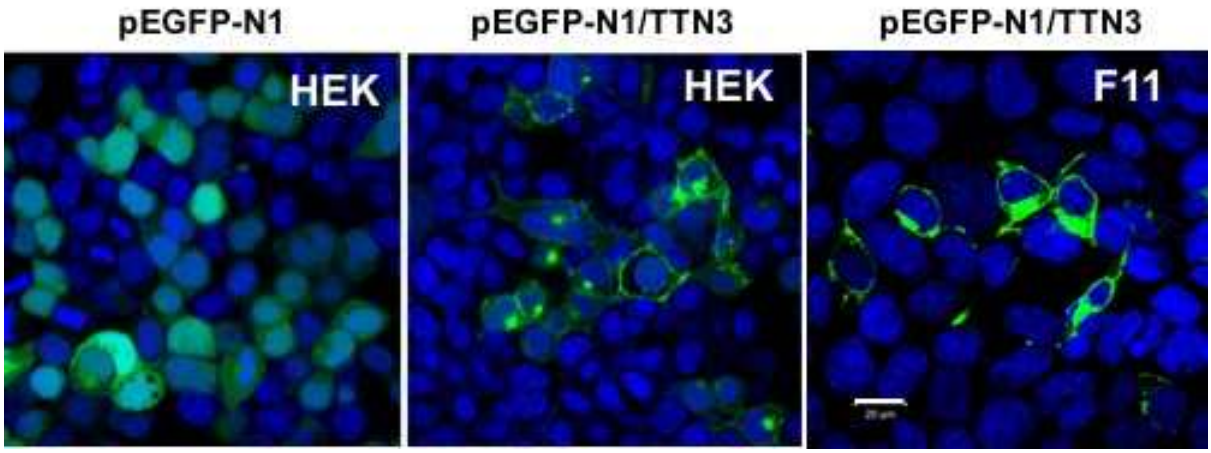

Figure S2.

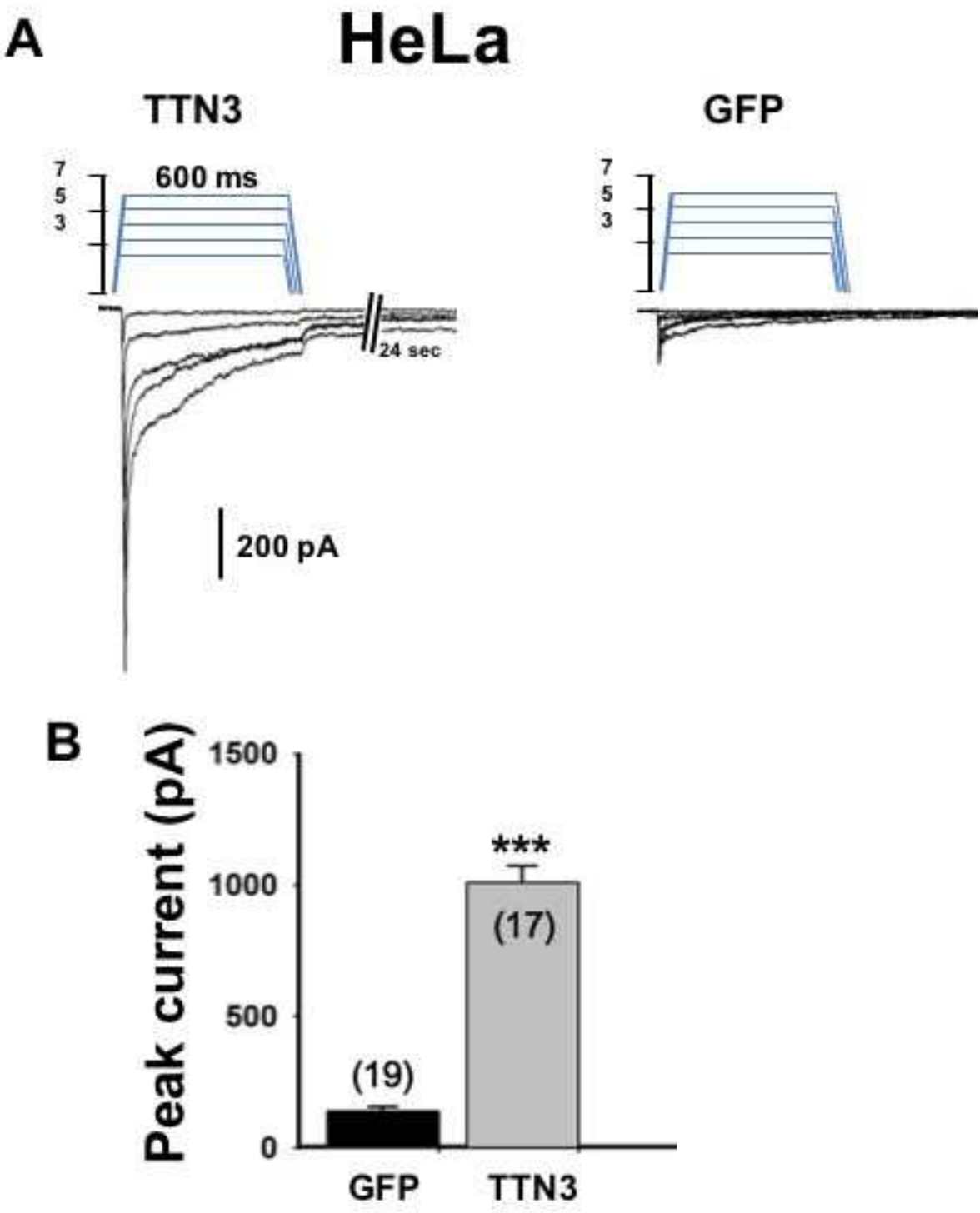
A
HeLa
TTN3
GFP
7
5
3
600 ms
24 sec
200 pA
B
Peak current (pA)
1500
1000
500
0
***
(17)
(19)
GFP
TTN3

Figure S3.

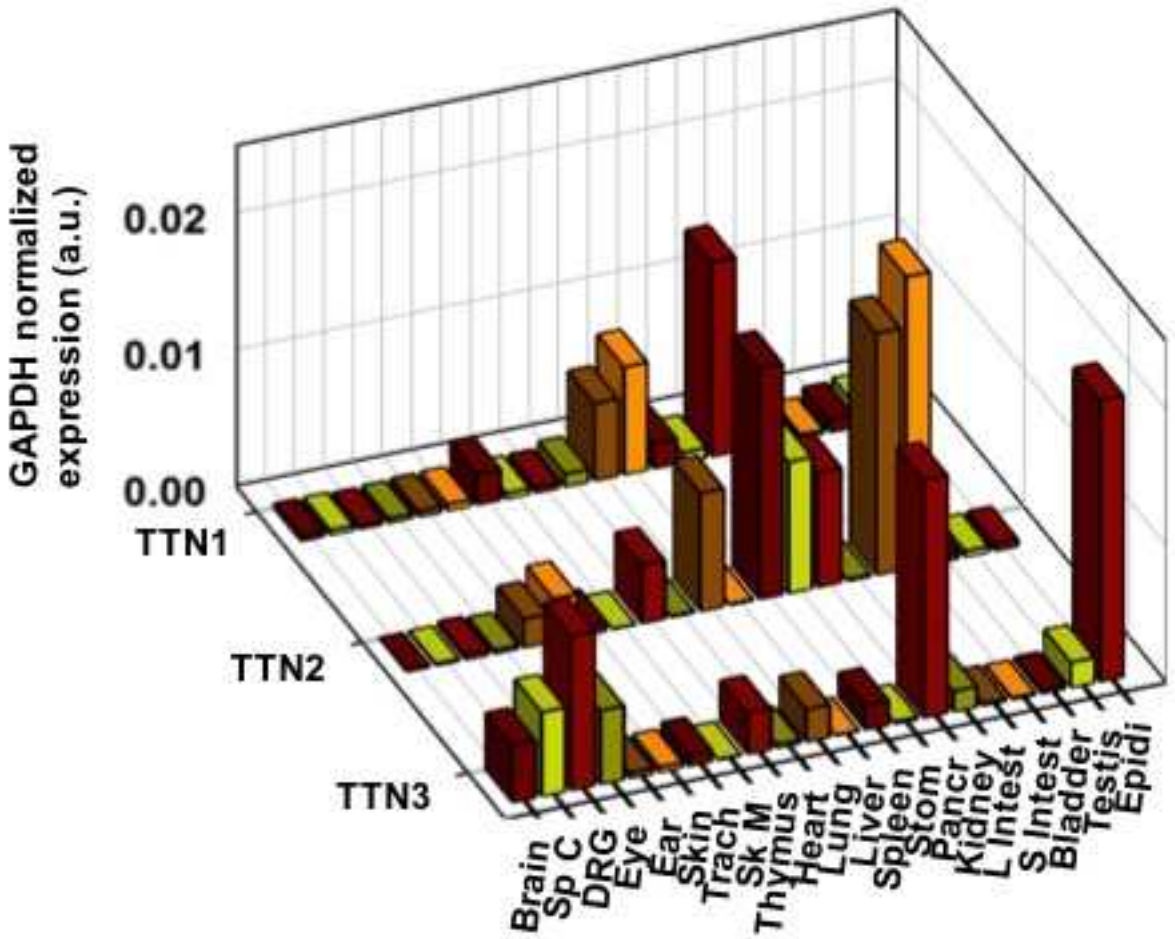
GAPDH normalized expression (a.u.)
0.02
0.01
0.00
TTN1
TTN2
TTN3
Brain
Sp C
DRG
Eye
Ear
Skin
Trach
Sk M
Thymus
Heart
Lung
Liver
Spleen
Stom
Pancr
Kidney
L Intest
S Intest
Bladder
Testis
Epidi

Figure S4.

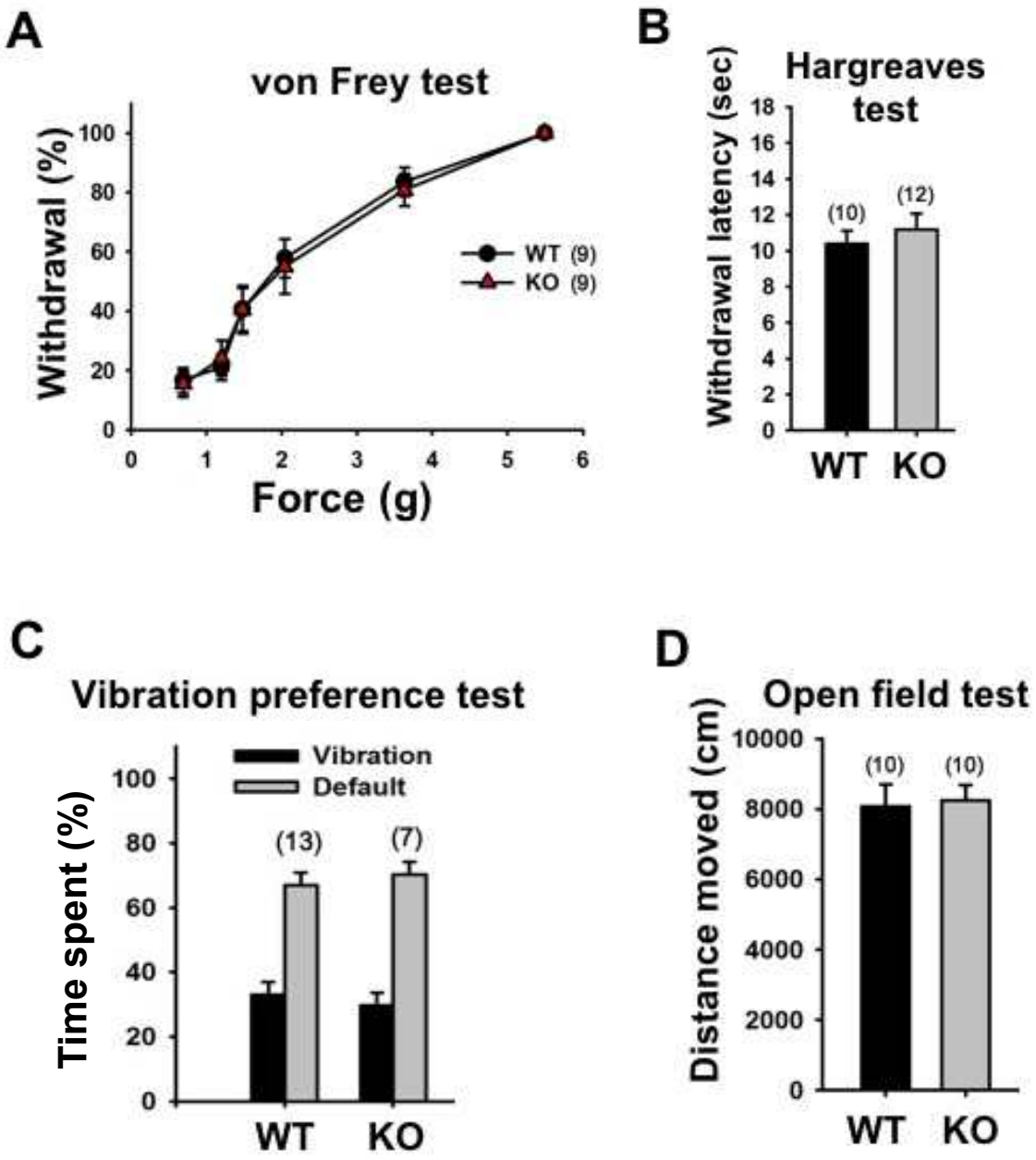
A
von Frey test
Withdrawal (%)
Force (g)
WT (9)
KO (9)
B
Hargreaves test
Withdrawal latency (sec)
(10)
(12)
WT
KO
C
Vibration preference test
Time spent (%)
Vibration
Default
(13)
(7)
WT
KO
D
Open field test
Distance moved (cm)
(10)
(10)
WT
KO

Table S1.

Protein Acc.	Gene	*Organism*	
NP_001073975.1	*Ttn3*	*H. sapiens*	Human
NP_878261.1	*Ttn3*	*M. musculus*	mouse
NP_001101824.1	*Ttn3*	*R. norvegicus*	rat
XP_420558.4	*Ttn3*	*G. gallus*	chicken
XP_005155606.1	*Ttn3*	*D. rerio*	zebrafish
XP_002936503.1	*Ttn3*	*X. tropicalis*	frog
XP_007065696.1	*Ttn3*	*C. mydas*	turtle
XP_003985286.1	*Ttn3*	*F. catus*	cat
NP_001026908.1	*Ttn1*	*H. sapiens*	human
NP_659165.1	*Ttn1*	*M. musculus*	mouse
NP_620807.1	*Ttn1*	*R. norvegicus*	rat
XP_421633.3	*Ttn1*	*G. gallus*	chicken
NP_001038875.1	*Ttn1*	*D. rerio*	zebrafish
NP_001016894.1	*Ttn1*	*X. tropicalis*	frog
XP_007069920.1	*Ttn1*	*C.mydas*	turtle
XP_003984259.1	*Ttn1*	*F. catus*	cat
NP_001268940.1	*Ttn2*	*H. sapiens*	human
NP_001136264.1	*Ttn2*	*M. musculus*	mouse
NP_001100946.1	*Ttn2*	*R. norvegicus*	rat
NP_001032458.1	*Ttn2*	*D. rerio*	zebrafish
NP_001015997.1	*Ttn2*	*X. tropicalis*	frog
XP_003997471.1	*Ttn2*	*F. catus*	cat